



Frolova Liliia [eejet@entc.com.ua](mailto:eejet@entc.com.ua) [lewat journals.uran.ua](http://journals.uran.ua)  
kepada saya ▾

Sab, 12 Des 2020, 14.41 ☆ ↶ ⋮

🇺🇦 Ukraina ▾ > Inggris ▾ [Terjemahkan pesan](#)

Nonaktifkan untuk: Ukraina ✕

Mr Adi Subardi:

Thank you for submitting the manuscript, "STRUCTURAL CHARACTERIZATION, OXYGEN CONTENT, AND CELL PERFORMANCE OF THE DOUBLE PEROVSKITE OXIDE FOR IT-SOFC CATHODE" to «Eastern-European Journal of Enterprise Technologies».

With the online journal management system that we are using, you will be able to track its progress through the editorial process by logging in to the journal web site:

Manuscript URL: <http://journals.uran.ua/eejet/author/submission/218760>  
Username: subardi\_1969  
Temporary Password: 123456789

If you have any questions, please contact me. Thank you for considering this journal as a venue for your work.

Frolova Liliia  
Eastern-European Journal of Enterprise Technologies



Oksana Nikitina <[0661966nauka@gmail.com](mailto:0661966nauka@gmail.com)>  
kepada saya ▾

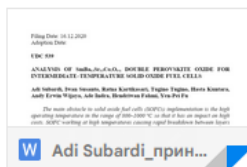
**An edited version of the article please provide no later than 24.03.2021.**

\*\*\*

--

\*\*\*

Satu lampiran • Dipindai dengan Gmail ⓘ



from "Eastern-European Journal of Enterprise Technologies" - Adi Subardi (stage 3, April) Kotak Masuk x



**Oksana Nikitina** <O661966nauka@gmail.com>

kepada saya, lwan, ratna, tugino, hasta, adeindra, hendriwan\_f, ypfu ▾

4 Jan 2021, 14.47



Good afternoon, dear Adi Subardi.

The article was accepted for consideration of the possibility of publication in (No. 2 (110).2021).

At the 3 - stage of editing, please take into account the comments of the editor (article in the application, color notes are highlighted).

WE ASK YOU TO RIGHT STRICTLY IN THE OPTION WHICH IS IN THE APPENDIX (see appendix).

We ask you not to delete the comments so that we can see all your edits. All corrections by the author, please highlight in green.

Please provide an edited version of the article **by 08.01.2021**.

We are in touch 24/7.

with respect, General manager  
Oksana Nikitina

---

Filing Date: 16.12.2020

Adoption Date:

UDC 539

## CHARACTERIZATION OF STRUCTURAL, OXYGEN CONTENT, AND CELL PERFORMANCE OF THE DOUBLE PEROVSKITE OXIDE

From the title should follow what your research was: development, comparison, implementation, research, analysis, etc.

**Adi Subardi, Iwan Susanto, Ratna Kartikasari, Tugino Tugino, Hasta Kuntara, Andy Erwin Wijaya, Ade Indra, Hendriwan Fahmi, Yen-Pei Fu**

*The main obstacle to solid oxide fuel cells (SOFCs) implementation is the high operating temperature in the range of 800 °C–1000°C so that it has an impact on high costs. SOFC working at high temperatures causing rapid breakdown between layers (anode, electrolyte, and cathode) because it has a different thermal expansion. The study focused on reducing the operating temperature in the medium temperature range.  $\text{SmBa}_{0.5}\text{Sr}_{0.5}\text{Co}_2\text{O}_{5+\delta}$  (SBSC) oxide was studied as a cathode material for IT-SOFCs base on  $\text{Ce}_{0.8}\text{Sm}_{0.2}\text{O}_{1.9}$  (SDC) electrolyte. The SBSC powder was prepared using the solid-state reaction method with repeated ball-milling and calcining. Alumina grinding balls are used because they have a high hardness to crush and smooth the powder of SOFC material. The specimens were then tested as cathode material for SOFC at intermediate temperature (600 °C–800°C) using X-ray powder diffraction (XRD), thermogravimetric analysis (TGA), electrochemical, and Scanning electron microscopy (SEM) tests. The X-ray powder diffraction (XRD) pattern of SBSC powder can be indexed to a tetragonal space group (P4/mmm). The overall change in mass of the SBSC powder is 8% at a temperature range of 125 °C–800 °C. A sample of SBSC powder showed a high oxygen content ( $5+\delta$ ) that reached 5.92 and 5.41 at temperatures of 200 °C and 800 °C, respectively. High diffusion levels and increased surface activity of oxygen reduction reactions (ORRs) can be affected by high oxygen content ( $5+\delta$ ). The polarization resistance ( $R_p$ ) of samples sintered at 1000°C is 4.02  $\Omega\text{cm}^2$  at 600 °C, 1.04  $\Omega\text{cm}^2$  at 700 °C, and 0.42  $\Omega\text{cm}^2$  at 800 °C. The power density of the SBSC cathode is 336.1, 387.3, and 357.4  $\text{mW/cm}^2$  at temperatures of 625 °C, 650°C, and 675 °C, respectively. The SBSC demonstrates as a prospective cathode material for IT-SOFC*

*Keywords: Solid oxide fuel cell; Thermal properties; Oxygen content; Electrochemical properties; Cell performance*

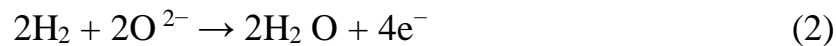
### 1. Introduction

Limited fossil fuels and global warming are increasingly threatening human survival and have been serious global issues for decades. New power plants using fuel sources such as solid oxide fuel cells (SOFCs) have attracted much attention around the world, and the technology is expected to reduce obstacles in the supply of electricity in the future. The advantage of SOFCs compared with other types of fuel

cells is that they are a more efficient and flexible fuel source. SOFCs also offer low pollutant emissions because the final stage of their usage only produces a vapor or hot water [1–3]. The schematic diagram exhibiting the basic operation of SOFC is shown in Fig. 1, *a*. At the cathode side, the oxygen reduction reaction occurs by accepting electrons from the external circuit. The reactions can be written below:



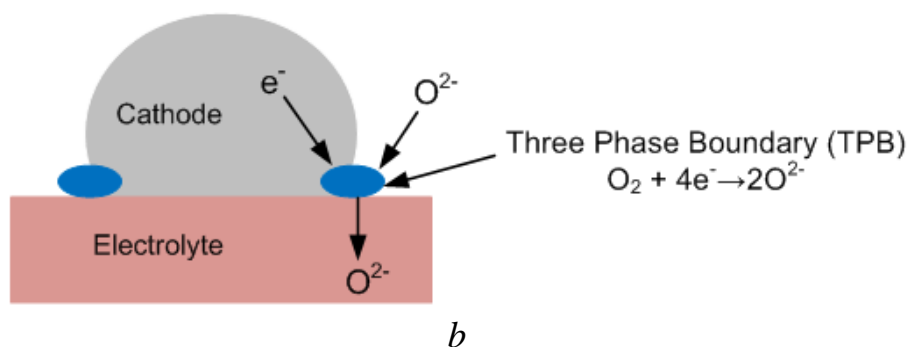
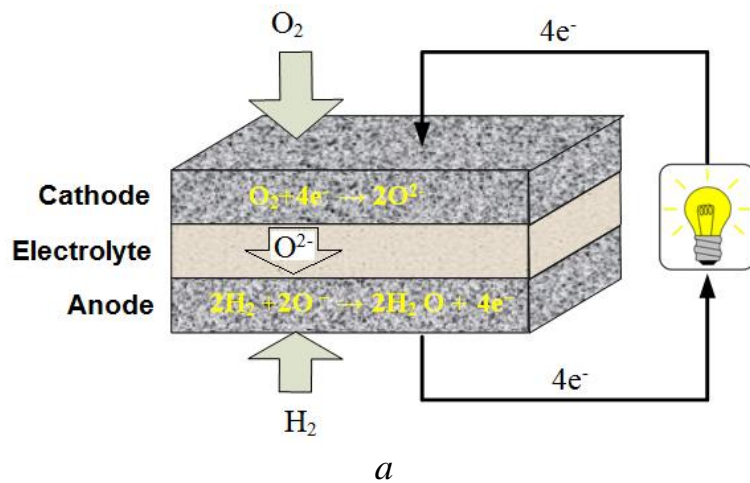
The produced oxide ions ( $\text{O}^{2-}$ ) pass through the electrolyte to the anode side and combine with the protons produced by the oxidation of hydrogen or other fuels to produce water. The reactions can be written:



Overall reaction,



This reaction occurs at the three-phase boundary (TPB) [4]. The TPB is the interfacial area among electrode, electrolyte, and gaseous fuel where the overall reaction occurs (Fig. 1, *b*). The electrons flowing from the anode to the cathode produce electrical work in the “Load”.



## Sign by example:

Fig. 2. The main signature: *a* - .....; *b* - .....

Fig. 1. (a) Schematic diagram of SOFC operation, and (b) diagram exhibiting three-phase boundary (TPB)

Through the process, chemical energy is directly converted to electrical energy. To increase the active area where the oxygen reduction reaction (cathode) or hydrogen oxidation reaction (anode) occurs, a porous electrode structure is employed. Meanwhile, the dense electrolyte provides a physical barrier to prevent the direct mixing of fuel and air.

## 2. Literature review and problem statement

In general, traditional SOFCs operate at high temperatures, which causes several problems including high production costs, mismatches in thermal expansion between the fuel cell components, and chemical compatibility. Therefore, current research is focused on SOFCs that can operate at lower temperatures (400 °C–800 °C) and aims to reduce production costs and achieve a long working lifetime (40,000 h) [5, 6]. Lower operating temperatures cause the catalytic activity of the electrodes to decrease significantly, and the cathode is a limiting factor for overall fuel cell performance. Therefore, the focus is being directed toward maintaining stability in the cathode material and increasing the high electrochemical performance of IT-SOFCs. In other words, a vital result of the research into fuel cell performance is the discovery that the cathode polarization can be eliminated [7]. However, the application of SOFC is widely constrained due to the impact of low catalytic activity on the oxygen reduction reactions (ORRs) at the cathode. Mixed ionic-electronic conductor cathodes (MIECs) are successful in increasing the active ORR zone from the three-phase boundary to the cathode-gas interface site, which will reduce cathodic resistance [7, 8]. The ORR site of MIECs works on the TPB (the electrolytes, cathodes, and gas phases) and at the two-phase boundary between the gas phase and the cathode [9].

Recently, among the various MIECs oxides, cobalt-containing perovskite oxides such as  $\text{SmBa}_{0.6}\text{Sr}_{0.4}\text{Co}_2\text{O}_{5+\delta}$  [10],  $\text{PrBa}_{0.5}\text{Sr}_{0.5}\text{Co}_{2-x}\text{Fe}_x\text{O}_{5+\delta}$  [11],  $\text{NdBa}_{1-x}\text{Sr}_x\text{Co}_2\text{O}_{5+\delta}$  [12],  $\text{YBa}_{0.6}\text{Sr}_{0.4}\text{Co}_2\text{O}_{5+\delta}$  [13], and  $\text{GdBa}_{0.5}\text{Sr}_{0.5}\text{Co}_{2-x}\text{Fe}_x\text{O}_{5+\delta}$  [14] have attracted strong interest due to their electrocatalytic activity performance for the ORR. Also, the investigation has been conducted for layered perovskites with the chemical formula  $\text{LnBaCo}_2\text{O}_{5+\delta}$  (Ln-selected lanthanides) [15–22]. Several research groups also have investigated the electrochemical properties of a new type of MIEC oxide, cation ordered  $\text{LnBaCo}_2\text{O}_{5+\delta}$  (Ln = La, Pr, Sm, Gd, Y), as a potential cathode material for IT-SOFCs. Cobalt in cathodes is beneficial for the activation of oxygen reduction and thus provides a lower activation polarization loss. Cobalt-based cathodes, however, have high TECs because of the low-spin to the high-spin transition of Co. The incompatibility in thermal expansion can cause thermal stress in SOFCs and thus result in poor long-term thermal stability [12]. Therefore, it is important to improve the thermal expansion compatibility between the cathodes and the electrolytes. Zhou *et al.* [23] have declared that  $\text{LnBaCo}_2\text{O}_{5+\delta}$  cathodes with an intermediate lanthanide-

ion radius, such as  $\text{Sm}^{3+}$ , may provide a compromise between the values of the catalytic activity and thermal expansion coefficients. Recent reports exhibit when A' site is partially substituted by Sr, it could potentially improve the conductivity of double perovskite oxides where Sr-doped oxide  $\text{YBa}_{0.5}\text{Sr}_{0.5}\text{Co}_2\text{O}_{5+\delta}$  demonstrated excellent conductivity values (about 32 times higher than that of the Sr-free sample). Moreover, the Sr-doped layered perovskite oxide system  $\text{LnBa}_{0.5}\text{Sr}_{0.5}\text{Co}_2\text{O}_{5+x}$  ( $\text{Ln} = \text{Pr}, \text{Sm}, \text{and Gd}$ ), which showed a lower polarization resistance based on doped ceria electrolyte [24]. However, observations of SOFC performance in the range of 625, 650, and 675 °C have not been experimentally investigated. From the research reported above, some of the obstacles that SOFC faced were high working temperatures and high thermal expansion differences in SOFC components. Efforts were made to overcome this problem, the use of SBSC material as a cathode is expected to reduce the working temperature of SOFC so that the compatibility of SOFC components meets the requirements. In this work, SBSC oxide is synthesized, and aspects of its structural characteristics, thermal and electrochemical performance, power density, and microstructure are investigated. The SBSC oxygen reduction mechanism is also observed under various oxygen partial pressures (OPPs).

### **3. The aim and objectives of the study**

The study aims are to investigate the characteristics of double perovskite oxide ( $\text{SmBa}_{0.5}\text{Sr}_{0.5}\text{Co}_2\text{O}_{5+\delta}$ ) cathode for intermediate temperature solid oxide fuel cells (IT-SOFCs). The steps to achieve this goal through (a) Use of Samarium ( $\text{Sm}^{3+}$ ) to decline the operating temperature over the range of 600 °C–800 °C using a conventional technique (solid-state reaction), (b) SDC is used as an electrolyte layer, and (c) Observation and testing of composite SOFC oxide consisting of Ni-SDC layers SDC|SBSC

### **4. Materials and methods for preparing and testing specimens**

The material synthesis methods for the cathodes and electrolytes are described in previously published papers [25, 10]. The SBSC cathode powder was prepared using a solid-state reaction technique. The stoichiometric amounts of cathode material ( $\text{Sm}_2\text{O}_3$ ,  $\text{BaCO}_3$ ,  $\text{SrCO}_3$ , and  $\text{CoO}$ ) were ball-milled in ethanol for 12 h. The slurry was then heated at a temperature of 1000 °C in the air for six h. The  $\text{Ce}_{0.8}\text{Sm}_{0.2}\text{O}$  (SDC) powder was synthesized using the coprecipitation technique using the precursor materials  $\text{Ce}(\text{NO}_3)_3 \cdot 6\text{H}_2\text{O}$  and  $\text{Sm}(\text{NO}_3)_3 \cdot 6\text{H}_2\text{O}$ . A stoichiometric ratio applied, distilled water was then used to dissolve the starting material before being added to the ammonia solution.

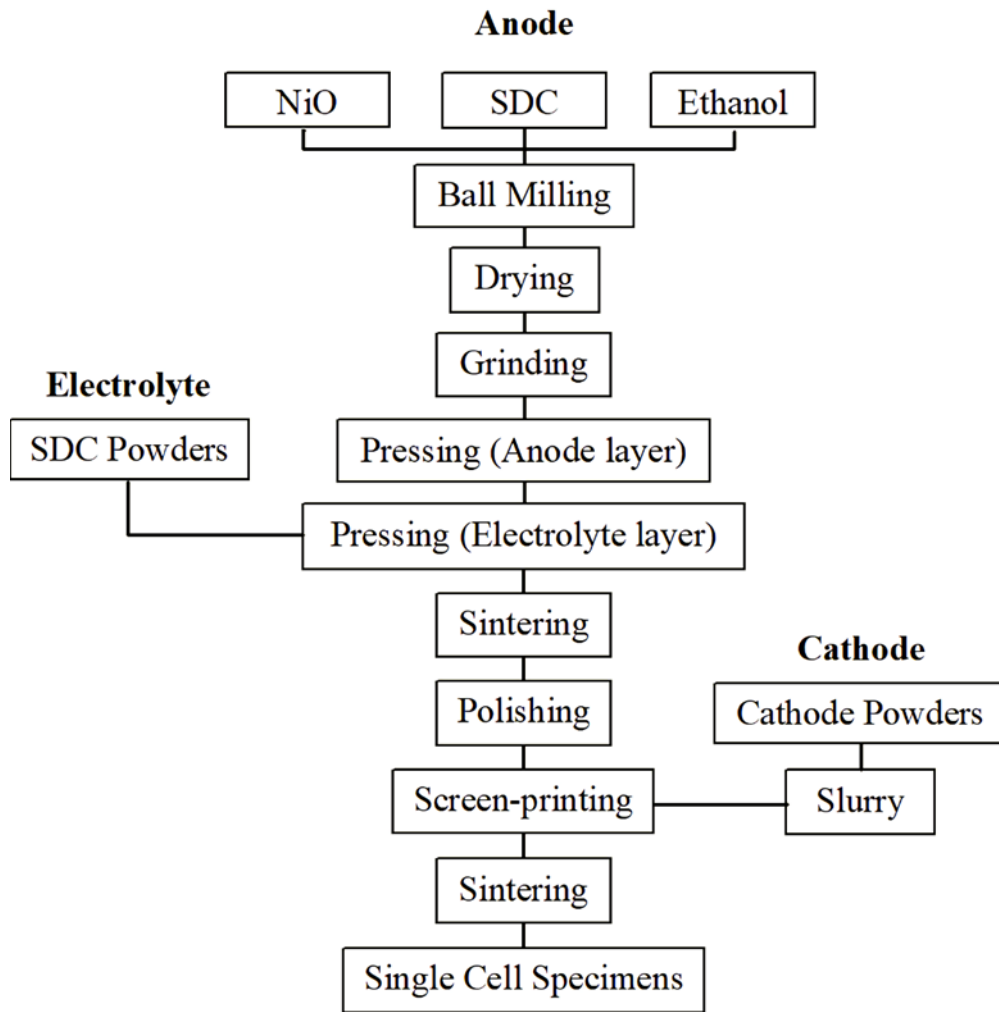


Fig. 2. The procedure of preparation for single-cell specimens

The pH value ranging from 9.5 to 10 is applied to the mixed solution. The precipitate was washed three times after it was filtered using distilled water and ethanol. In the next process, the coprecipitation powder was heated at 600 °C and held in the air for two h. For a binding agent, a small amount of polyvinyl alcohol (PVA) was mixed into the SDC powder and then pelletized to dimensions of 1.5 cm in diameter and 0.1 cm in thickness using uniaxial pressure applied at 1000 kg f/cm<sup>2</sup>. The disk-shaped sample was heated at 1500 °C and held for five h, followed by cooling to room temperature [25]. The procedure stages of fabricating a single cell specimen, as presented in Fig. 2. The structure of the SBSC cathode powder was observed by XRD using a Rigaku D/MAX-2500V, the radiation source of a Cu K $\alpha$  (1.5418 Å), and a scanning range of 10°–80°. To explain the lattice parameter and powder pattern for the sample, we used the GSAS program to perform a Rietveld refinement. The SBSC cathode microstructure (top view) and the cross-sectional image of the symmetrical cell were investigated by SEM (a Hitachi 3400N). The TG/DTA 6300 was used to analyze the thermogravimetric behavior of SBSC cathodes in the air (100 cm<sup>3</sup>/min). The oxygen content was calculated using the following formula:



$$\delta = \frac{M_s \Delta m}{M_o m} \quad (4)$$

The abbreviations/symbols in the formula are explained as follows, *the specimen molar mass ( $M_s$ )*, *the specimen mass in the air at room temperature ( $m$ )*, and *the molar mass of oxygen ( $M_o$ )* [26]. The cathode paste of SBSC involves cathode powder, the binding agent, a plasticizer, and a solvent, all of which were conducted by ball-mill processes. Screen printing technique was used to prepare a half cell sample of SBSC|SDC|SBSC. The manufacturing details of the half-cell sample are discussed in an earlier paper. The symmetrical cell testing was carried out under air in temperatures ranging from 600 °C to 800 °C in a furnace. The AC impedance measurement was performed using the VoltaLab PGZ301 potentiostat with a frequency applied range from 100 kHz to 0.1 Hz with 10 mV AC signal amplitude. The EIS fitting analysis was performed with the Z-view software [27]. The digital source meter (Keithley 2420) was used to collect Voltage (V) - current (I) from a single cell in the temperature range between 625 °C and 675 °C. Button cells were measured with humidified hydrogen (3 vol% H<sub>2</sub>O) as the fuel and air as the oxidant. The configuration of the single-cell sample was Ni-SDC|SDC|SBSC with a 1.3 cm diameter. In a preceding paper [28], the detailed stages for preparing a single cell are given.

## 5. Results

### 5. 1. Structure of Crystal

The crystal structure and phase composition of the SBSC powder were observed using X-ray diffraction (XRD). From software GSAS analysis, characteristic XRD peaks were detected as double perovskite oxide. The peaks caused by impurities are not detected in the structure of SBSC, which indicates a well-prepared sample. Meanwhile, the lattice parameters are obtained:  $a = 3,861 \text{ \AA}$ ,  $b = 3,861 \text{ \AA}$ ,  $c = 7,617 \text{ \AA}$ , and  $v = 113.56 \text{ \AA}^3$ , with reliability factors of  $R_{wp} = 0.41$  and  $R_p = 0.23$ . In this structure, Sm atoms are in position 1a, Sr, and Ba atoms are randomly distributed at position 1b.

Before the table should be a link to the table (in the same section)

**Table 1**

Crystallographic data at room temperature for SBSC. Cell parameters were collected using a Rietveld refinement

Atom	Wyckoff position	x	y	z	Uiso	Occ
Sm	1a (0 0 0)	0	0	0	0.0333	0.8797
Co	2h (½ ½ z)	1/2	1/2	0.25592	0.0045	0.9944
Ba/Sr	1b (0 0 ½)	0	0	1/2	0.0092	0.8926
O1	4i (0 ½ z)	0	1/2	0.26780	0.0077	0.9311
O2	1c (½ ½ 0)	1/2	1/2	0	0.1906	1.2455



O3	2h ( $\frac{1}{2}$ $\frac{1}{2}$ z)	1/2	1/2	0.44110	0.0333	0.4220
----	-------------------------------------	-----	-----	---------	--------	--------

Meanwhile, the Co atom occupies position 2h (0.5,0.5,z). The SBSC structure has three kinds of oxygen atom sites: O3 at 2h (0.5,0.5,z), O2 at 1c (0.5,0.5,0), and O1 at 4i (0,0.5,z).

Fig. 3 shows the refinement of SBSC patterns including the measured XRD data, the calculated profile, and the difference between them. The refinement using the General Structure Analysis System (GSAS) program is typically used for crystallographic analysis, quantitative phase determination, texture mapping, stress-strain measurements, and other related types of materials characterization. The test results agree with the measured profiles, indicating that in the perovskite lattice, cations are well ordered.

Before the table should be a link to the table (in the same section)

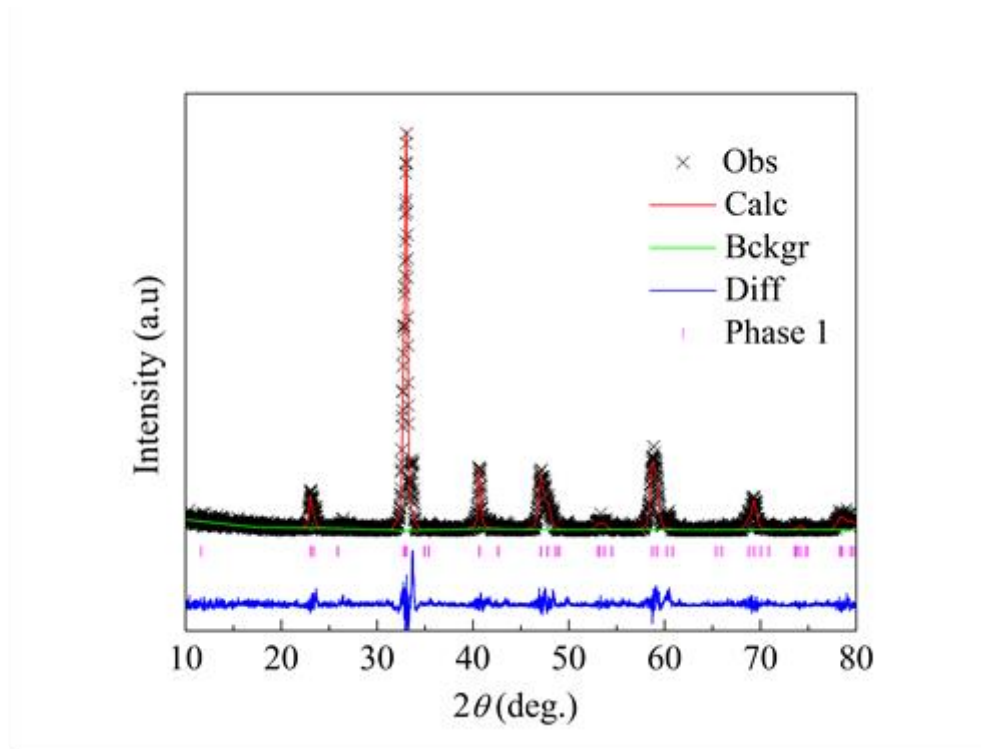


Fig. 3. Rietveld refinement data of the SBSC cathode at room temperature

Before the table should be a link to the table (in the same section)

Table 2

Space group, fractional coordinates, and lattice parameters of corresponding double perovskite structure cathodes.

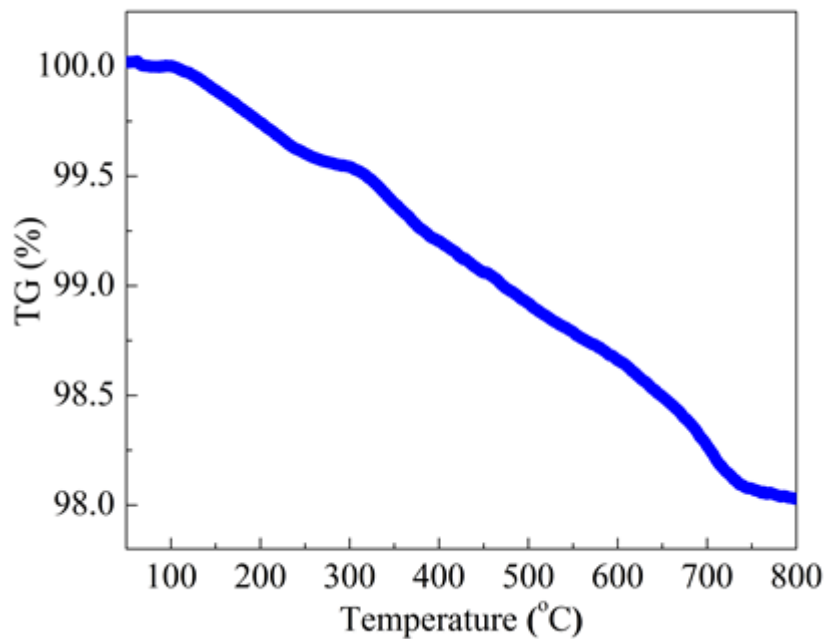
Specimens	Space group	a (Å)	b (Å)	c (Å)	V (Å <sup>3</sup> )	R <sub>wp</sub>
NdBaCo <sub>2</sub> O <sub>5+δ</sub> [29]	P4/mmm	3.903	3.903	7.614	116.02	0.42
SmBaCoO <sub>5+δ</sub> [29]	Pmmm	3.886	7.833	7.560	230.22	0.45

$\text{NdBa}_{0.5}\text{Sr}_{0.5}\text{Co}_2\text{O}_{5+\delta}$ [30]	P4/mmm	3.861	3.861	7.715	115.01	0.36
$\text{NdBa}_{0.5}\text{Sr}_{0.5}\text{Co}_{1.5}\text{Mn}_{0.5}\text{O}_{5+\delta}$ [31]	P4/mmm	3.855	3.855	7.705	114.54	0.12
$\text{SmBa}_{0.6}\text{Sr}_{0.4}\text{Co}_2\text{O}_{5+\delta}$ [10]	P4/mmm	3.870	3.870	7.590	114.11	0.29
$\text{SmBa}_{0.5}\text{Sr}_{0.5}\text{Co}_2\text{O}_{5+\delta}$ [32]	P4/mmm	3.883	3.883	7.580	114.30	0.28

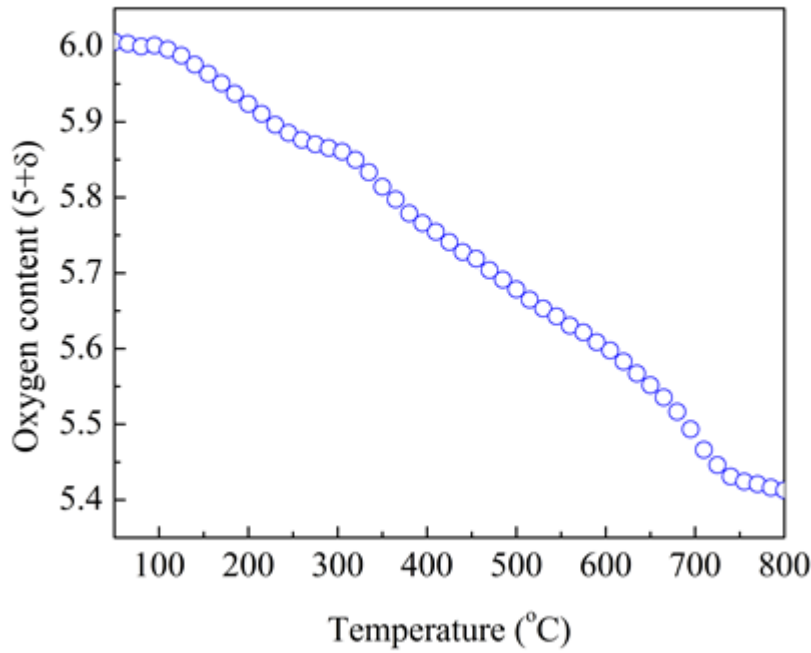
The SBSC cathode showed high structural stability when the samples were calcined under temperatures of 1000 °C and 1200 °C, which does not influence the crystal's structure [33]. The space group, fractional coordinates, and lattice parameters of corresponding double perovskite structure cathodes are shown in Table 2.

### 1.1. Thermal properties and oxygen content analysis

To clarify the oxygen content of the SBSC cathode, TGA was conducted in the air. The TGA curve indicates that the specimen had slight weight loss before 125 °C, which is associated with the desorption of the specimen's absorbed water as presented in Fig. 4, *a*. With a further increase in temperature, the magnitude of weight loss became significant and continued until weight loss slowed at temperatures of 250 °C–325 °C.



*a*



*b*

**Sign by example:**

Fig. 2. The main signature: *a* - .....; *b* - .....

Fig. 4. (a) The TGA curve of the SBSC powder over a temperature range between 27  $^{\circ}\text{C}$  and 800  $^{\circ}\text{C}$ , (b) the oxygen content ( $5+\delta$ ) as a function of temperature in air for SBSC cathodes

Above 325  $^{\circ}\text{C}$ , the rate of degradation in weight loss was significant, and the mass change slowed again at temperatures around 725  $^{\circ}\text{C}$ . It can be seen that from 650  $^{\circ}\text{C}$  to 750  $^{\circ}\text{C}$  the weight loss rate tends to increase. Then, at a temperature range of 750  $^{\circ}\text{C}$ , weight loss seems to slow down again until it reaches a temperature of 800  $^{\circ}\text{C}$ . Detailed oxygen content ( $5+\delta$ ) information as a function of temperature is listed in Table 3.

Table 3

The  $5+\delta$  as a function of temperature in air for the SBSC cathode

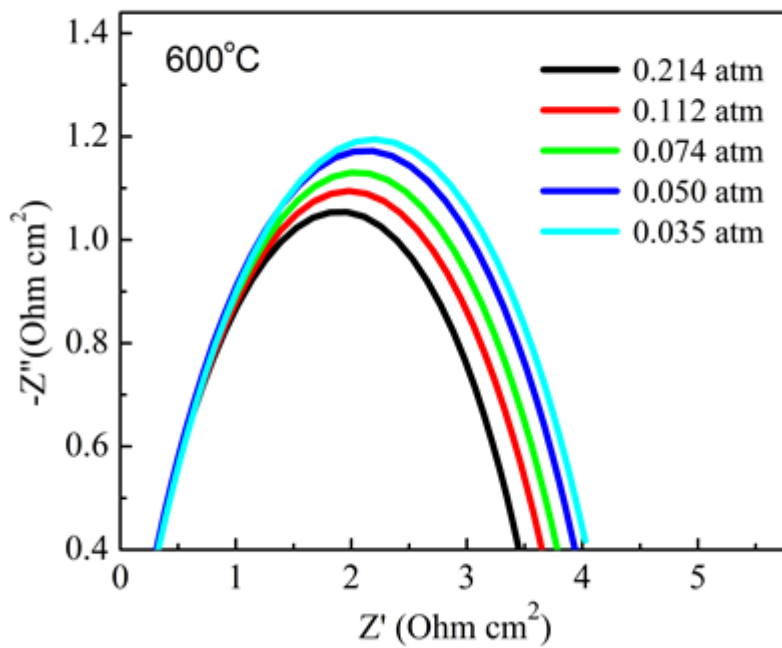
Specimens	Calcination temperature ( $^{\circ}\text{C}$ )	$5+\delta$			
		200 $^{\circ}\text{C}$	400 $^{\circ}\text{C}$	600 $^{\circ}\text{C}$	800 $^{\circ}\text{C}$
SBSC91 [24]	1200	5.53	5.44	5.32	5.18
SBSC73 [24]	1200	5.62	5.55	5.36	5.22
SBSC55 [24]	1200	5.74	5.64	5.51	5.39
SBSC [this work]	1000	5.92	5.76	5.60	5.41

The calcination temperature has an impact on the oxygen content of the SBSC cathode. The oxygen content of the cathode with a calcination temperature of 1200  $^{\circ}\text{C}$

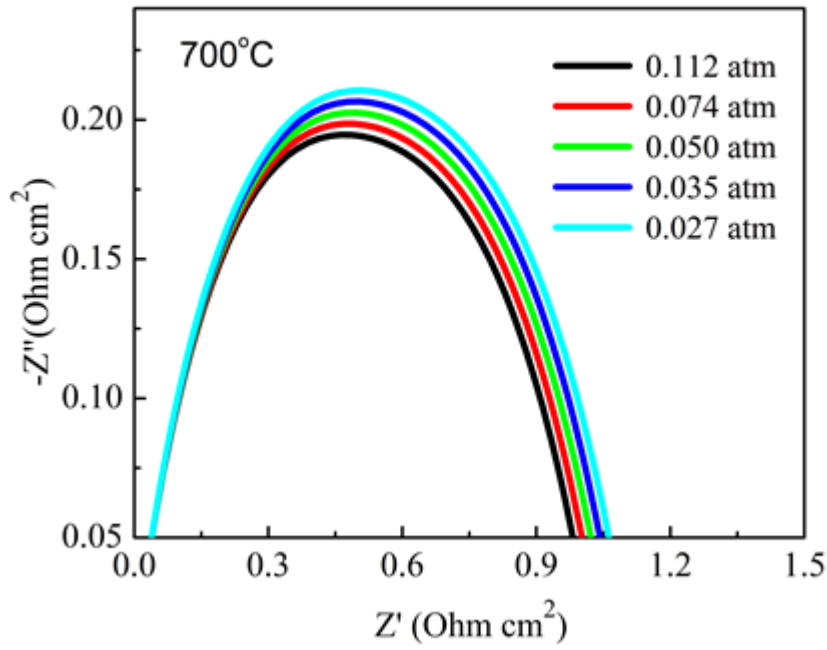
is smaller than that of a calcined at a temperature of 1000 °C. In the cathode with the calcination of 1200 °C , the oxygen content values were 5.74 (200 °C) and 5.39 (800 °C), while in the cathode with the calcination temperature 1000 °C the oxygen content values obtained were 5.92 and 5.41.

### 1.2. OPP Half-Cell

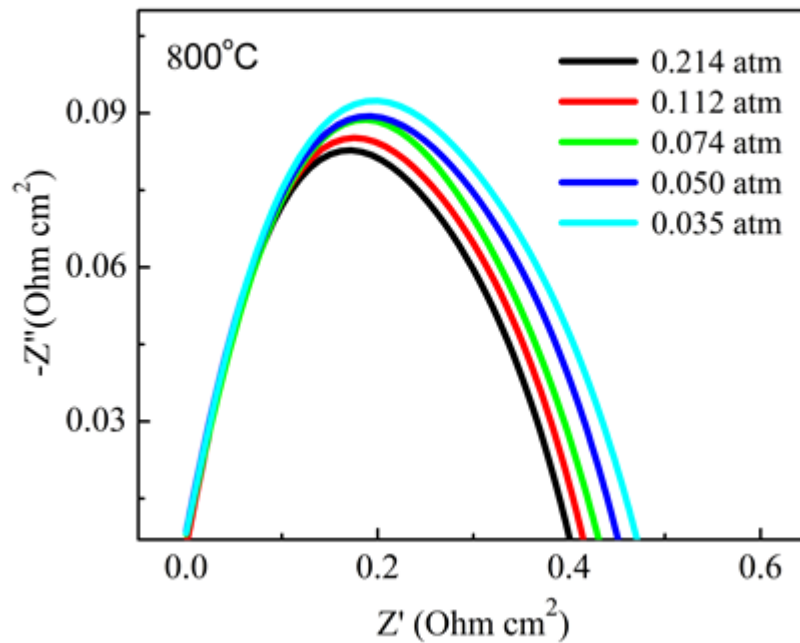
Typical impedance spectra for symmetrical cells (SBSC|SDC|SBSC) were obtained by AC impedance spectroscopy. Fig. 4 presents the polarization resistance ( $R_p$ ) values as a function of  $p(\text{O}_2)$ ; these were investigated under various temperatures between 600°C and 800°C and OPPs that ranged from 0.214 to 0.035 atm.



a



*b*



*c*

Sign by example:

Fig. 2. The main signature: *a* - .....; *b* - .....

Fig. 5. The fitting data of impedance spectra for symmetrical cells measured at (a) 600 °C, (b) 700 °C, and (c) 800 °C. The various OPPs from 0.214–0.035 atm.

The  $R_p$  values increased with decreasing  $p(\text{O}_2)$  values due to the decrease in mobile interstitial oxygen at lower  $p(\text{O}_2)$  values. The fitting of the impedance spectrum for symmetrical cells using the Z-View program.

Before the table should be a link to the table (in the same section)

**Table 4**

Interfacial polarization resistance ( $R_p$ ) as a function of  $p(\text{O}_2)$  for SBSC|SDC|SBSC symmetrical cells

$p(\text{O}_2)$ (atm)	$R_p$ ( $\Omega\text{cm}^2$ )		
	600°C	700°C	800°C
0.214	4.02	1.04	0.42
0.112	4.62	1.06	0.43
0.074	4.90	1.08	0.45
0.050	5.10	1.10	0.47
0.035	5.32	1.20	0.49

The cathode cell performance is influenced by the values of the  $R_p$  obtained from the components. The high  $R_p$  values have a significant impact on SOFC performance. In general, the value of  $R_p$  has decreased with the increase in the working temperature of the SOFC. These conditions, the manufacture of SOFC components, especially the high density between layers (anode, electrolyte, and cathode), is of great concern to researchers.

### 1.3. Single-Cell Performance

Fig. 6 shows the single-cell performance of anode-supported Ni-SDC|SDC|SBSC was performed under air/humidified hydrogen (3 vol%  $\text{H}_2\text{O}$ ). Increasing temperature has an impact on increasing the current density and power density due to the thermally activated kinetic process [34]. Due to the same phenomenon, cell voltage increased at higher temperatures. Fig. 4 also indicates that the open-circuit voltages (OCVs) are 0.83, 0.81, and 0.84 at 425 °C, 450 °C, and 475 °C, respectively; these values are lower than the theoretical values.

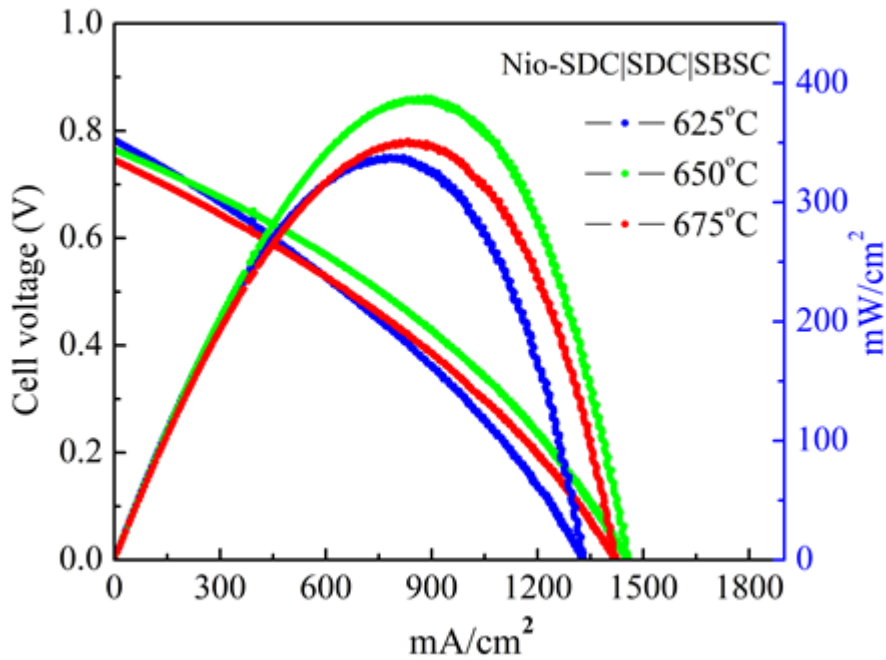


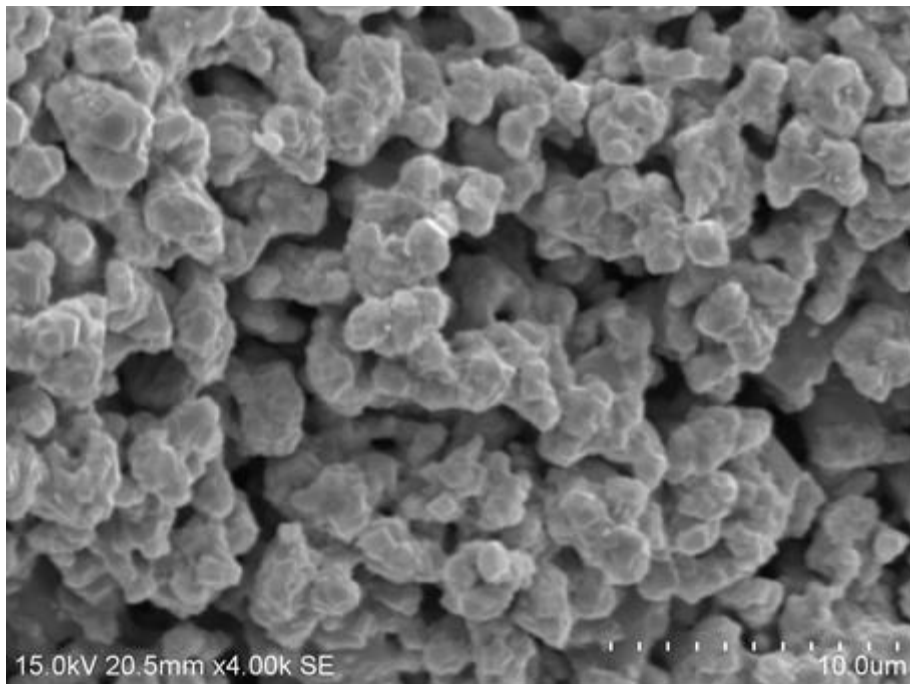
Fig. 6. The performance of a single cell of Ni-SDC|SDC|SBSC at temperatures ranging from 625 °C to 725 °C

The cathode performance in the SOFC cell as shown in Fig. 6, the power density at 650 °C exceeds that of the cell at 675 °C. This phenomenon needs to be analyzed more deeply because in general, the performance of SOFC cells increases with an increased operating temperature range between 600 °C and 800 °C. With these results, it can be stated that the SBSC oxide works well as a SOFC cathode at intermediate operating temperature.

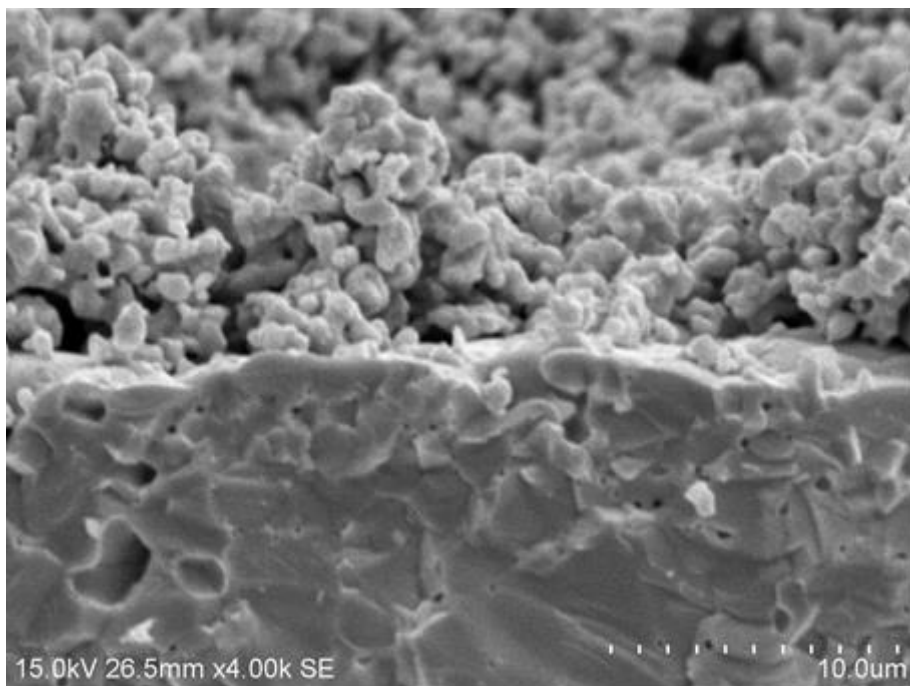
### 5. 5. SEM Image

In the symmetric cell, the cathode layer of SBSC was calcined in air for two h at 1000 °C. A uniform porous microstructure facilitates the gas diffusion of the cathode layer. A well-connected electrolyte–cathode interface determines low resistance in the solid oxide fuel cell.





*a*



*b*

**Sign by example:**

**Fig. 2. The main signature: *a* - .....; *b* - .....**

Fig. 7. (a) Cross-sectional SEM image of the SBSC cathode in the SBSC|SDC|SBSC symmetrical cell specimen prepared at 1000 °C for two h, and (b) a top view of the SBSC cathode

In Fig. 7, *b*, the adhesion between the SDC electrolyte and the SBSC cathode layer is quite good. The SBSC cathode grain size is distributed uniformly in the range

of 1.5–2  $\mu\text{m}$  and is porous.

## 2. Discussion of experimental results

The XRD pattern of SBSC powder, which can be categorized into a tetragonal space group (P4/mmm) is as shown in Fig. 3, after calcining at 1000 °C for six h. There is a good compatibility level between the experimental data and calculated profiles, which shows that the cations are ordered well in the perovskite lattice arrangement between the  $\text{Sm}^{3+}$  and  $\text{Ba}^{2+}/\text{Sr}^{2+}$  ions [35]. The cell parameters regarding the SBSC cathode structure collected from Rietveld refinement are described in Table 1.

The overall change in mass of the SBSC powder reached 8% at temperatures of 125 °C–800 °C. Previous data showed that the specimen was beginning to lose oxygen lattices significantly at a specific temperature [36]. A partial loss of oxygen lattices, along with a reduction in  $\text{Co}^{3+}$  to  $\text{Co}^{2+}$ , or  $\text{Co}^{4+}$  to  $\text{Co}^{3+}$ , and an increase in temperature, causes a decrease in weight loss during heating. Therefore, the oxygen content decreases with temperature [37,38]. The high diffusivity regarding oxide ions and the increased surface activity of the ORRs might be due to a high oxygen content [39].

To clarify the polarization of the SBSC cathode resistance, the symmetrical cells test was carried out with various OPPs from 0.214–0.035 atm. From data, with increasing temperatures, the  $R_p$  values fell dramatically, suggesting that the SBSC sample ORR is a thermally activated process. The  $R_p$  values of the specimen reduced from 4.02  $\Omega\text{cm}^2$  at 600 °C to 0.42  $\Omega\text{cm}^2$  at 800 °C with an OPP of 0.214 atm as presented in Table 4. However, the  $R_p$  values increased significantly with a decreasing oxygen partial pressure. For instance, as the  $p(\text{O}_2)$  decreases from 0.214 to 0.035 atm, the  $R_p$  value increases from 4.02 to 5.32  $\Omega\text{cm}^2$  at a temperature of 600 °C. This study is consistent with results previously reported by Meng et al. regarding changes in polarization resistance to oxygen partial pressure [40]. The  $R_p$  values reflect cathodic behavior, including diffusion of oxygen at high temperatures in the gas phase, low-temperature ORR, and the surface of bulk diffusion/oxygen [41].

From single cell testing, ideally, the OCV of a cell should be similar to its 1.1 V theoretical value and should only small if affected by factors of operating conditions. Porosity impacts the leakage current when fuel/oxidants crossing the electrolyte membrane can cause low OCV values. The following equation can explain the concept of chemical defect:



Electrolyte-based materials with low electronic conductivity, such as SDC, may lead to a slight electron cross flow via the electrolyte. Alternatively,  $\text{Ce}^{4+}$  in SDC electrolytes is quickly reduced to  $\text{Ce}^{3+}$ , particularly at higher temperatures [29]. The power density values of the cell with an SBSC cathode are 336.1, 387.3, and 357.4  $\text{mW}/\text{cm}^2$  at 625 °C, 650 °C, and 675 °C, respectively. One method of improving cell performance is by modifying the cathode surface using electrolyte-based materials

such as SDC. As previously reported, SDC nanoparticles implanted into the porous surface of the cathode produce a significant increase in the power density value [42].

Fig. 7 shows a cross-sectional view of SBSC|SDC from the prepared symmetrical cell and top surface SEM images. The SBSC cathode grain size is distributed uniformly in the range of 1.5–2  $\mu\text{m}$  and is porous. Better morphology is very helpful to ensure increased current, reduced  $R_p$  values, and rapid oxygen diffusion during SOFC operations. Also, the cathode structure's properties determine the cell's performance in processes such as kinetic reactions, mass transportation pre-processes, and charge transportation [43].

## 7. Conclusions

1. The XRD structure of the SBSC cathode has been successfully categorized as double perovskite oxide by the solid-state reaction method. The double perovskite structure consists of the elements  $\text{Sm}^{3+}$ , Ba on the A-side and Sr, Co on the B side.

2. The  $R_p$  values of the specimen decreased from 4.02  $\Omega\text{cm}^2$  at 600  $^\circ\text{C}$  to 0.42  $\Omega\text{cm}^2$  at 800  $^\circ\text{C}$ . The maximum power density of the single cell is 387.3  $\text{mW}/\text{cm}^2$  at 650  $^\circ\text{C}$  indicates that SBSC qualifies as the SOFC cathode material.

3. SBSC cathodes show good performance at intermediate operating temperatures (600  $^\circ\text{C}$ –800  $^\circ\text{C}$ ).

## Acknowledgements

This work was supported by A113 Laboratory of MSE (NDHU) and grand funded through MOST 106-2113-M-259-011 by the Ministry of Science and Technology of Taiwan.

## References

- [1] B.C.H. Steele, A. Heinzl. (2001). Materials for fuel-cell technologies. *Nature*, 414, 345–352. doi.org/10.1038/35104620.
- [2] N.Q. Minh. (1993). Ceramic fuel cell. *J Am Ceram Soc.*, 76, 563–588. doi.org/10.1111/j.1151-2916.1993.tb03645.x.
- [3] J.C. Ruiz-Molares, D. Marrero-Lo'pez, J. Canales-Va'zquez, J.T.S. Irvine. (2011). Symmetric and reversible solid oxide fuel cells. *RSC Adv.*, 1, 1403–1414. doi.org/10.1039/c1ra00284h.
- [4] S.J. Skinner. (2011). Recent advances in perovskite-type materials for solid oxide fuel cell cathodes. *Int. J. Inorg. Mater.*, 3, 113–121. doi.org/10.1016/s1466-6049(01)00004-6.
- [5] D.J.L. Brett, A. Atkinson, N.P. Brandon, S.J. Skinner. (2008). Intermediate temperature solid oxide fuel cells. *Chem Soc Rev.*, 37, 1568–1578. doi.org/10.1039/b612060c .
- [6] H.Y. Liu, X.F. Zhu, M.J. Cheng, Y. Cong, W.S. Yang. (2011). Novel  $\text{Mn}_{1.5}\text{Co}_{1.5}\text{O}_4$  spinel cathodes for intermediate solid oxide fuel cells. *Chem Commun.*, 47, 2378–2380. doi.org/10.1039/c0cc04300a.
- [7] S.B. Adler. (2004). Factors governing oxygen reduction in solid oxide fuel cell cathodes. *Chem Rev.*, 104, 4791–4844. doi.org/10.1021/cr020724o.
- [8] Y. Takeda, R. Kanno, M. Noda, Y. Tomida, O. Yamamoto. (1987).

Cathodic polarization phenomena of perovskite oxide electrodes with stabilized zirconia. *Journal of The Electrochemical Society* volume, 134, 2656–2661. doi.org/10.1149/1.2100267.

[9] S.B. Adler, J.A. Lane, B.C.H. Steele. (1996). Electrode kinetics of porous mixed-conducting oxygen electrodes. *J Electrochem Soc.*, 143, 3554–3564. doi.org/10.1149/1.1837252.

[10] A. Subardi, M.H. Cheng, Y.P. Fu. (2014). Chemical bulk diffusion and electrochemical properties of  $\text{SmBa}_{0.6}\text{Sr}_{0.4}\text{Co}_2\text{O}_{5+\delta}$  cathode for intermediate solid oxide fuel cells. *Int J Hydrogen Energy*, 39, 20783–20790. doi.org/10.1016/j.ijhydene.2014.06.134.

[11] F. Zhao, S. Wang, K. Brinkman, F. Chen. (2010). Layered perovskite  $\text{PrBa}_{0.5}\text{Sr}_{0.5}\text{Co}_2\text{O}_{5+\delta}$  as high performance cathode for solid oxide fuel cells using oxide proton-conducting electrolyte. *J Power Sources*, 195, 5468–5473. doi.org/10.1016/j.jpowsour.2010.03.088.

[12] Q. Zhou, T. He, Y. Ji. (2008).  $\text{SmBaCo}_2\text{O}_{5+\delta}$  double-perovskite structure cathode material for intermediate-temperature solid-oxide fuel cells. *J Power Sources*, 185, 754–758. doi.org/10.1016/j.jpowsour.2008.07.064.

[13] A. Tarancon, M. Burriel, J. Santiso, S.J., Skinner, J.A. Kilner. (2010). Advances in layered oxide cathodes for intermediate temperature solid oxide fuel cells. *J Mater Chem.*, 20, 3799–3813. doi.org/10.1039/b922430k.

[14] D.J. Chen, R. Ran, K. Zhang, J. Wang, Z.P. Shao. (2009). Intermediate-temperature electrochemical performance of a polycrystalline  $\text{PrBaCo}_2\text{O}_{5+\delta}$  cathode on samarium-doped ceria electrolyte. *J Power Sources*, 188, 96–105. doi.org/10.1016/j.jpowsour.2008.11.045.

[15] C. Kuroda, K. Zheng, K. Swierczek. (2013). Characterization of novel  $\text{GdBa}_{0.5}\text{Sr}_{0.5}\text{Co}_{2-x}\text{Fe}_x\text{O}_{5+\delta}$  perovskites for application in IT-SOFC cells. *Int. J. Hydrogen Energy*, 38, 1027–1038. doi.org/10.1016/j.ijhydene.2012.10.085.

[16] A. Tarancon, A. Morata, G. Dezanneau, S.J. Skinner, J.A. Kilner, A. Estrade, F.H. Ramirez, F. Peiro, J.R. Morante. (2007).  $\text{GdBaCo}_2\text{O}_{5+\delta}$  layered perovskite as an intermediate temperature solid oxide fuel cell cathode. *J. Power Sources*, 174, 255–263. doi.org/10.1016/j.jpowsour.2007.08.077

[17] A. Chang, S.J. Skinner, J.A. Kilner. (2006). Electrical properties of  $\text{GdBaCo}_2\text{O}_{5+\delta}$  for SOFC applications. *Solid State Ionics*, 177, 2009–2011. doi.org/10.1016/j.ssi.2006.05.047.

[18] H. Gu, H. Chen, L. Gao, Y. Zheng, X. Zhu, L. Guo. (2009). Oxygen reduction mechanism of  $\text{NdBaCo}_2\text{O}_{5+\delta}$  cathode for intermediate-temperature solid oxide fuel cells under cathodic polarization. *Int. J. Hydrogen Energy*, 34, 2416–2420. doi.org/10.1016/j.ijhydene.2009.01.003.

[19] X. Kong, X. Ding. (2011). Novel layered perovskite  $\text{SmBaCu}_2\text{O}_{5+\delta}$  as a potential cathode for intermediate temperature solid oxide fuel cells. *Int. J. Hydrogen Energy*, 36, 15715–15721. doi.org/10.1016/j.ijhydene.2011.09.035.

[20] J.H. Kim, Y. Kim, P.A. Connor, J.T.S. Irvine, J. Bae, W. Zhou. (2009). Structural thermal and electrochemical properties of layered perovskite  $\text{SmBaCo}_2\text{O}_{5+\delta}$ , a potential cathode material for intermediate-temperature solid oxide fuel cells. *J. Power Sources*, 194, 704–711. doi.org/10.1016/j.jpowsour.2009.06.024.

[21] W. Liu, C. Yang, X. Wu, H. Gao, Z. Chen. (2011). Oxygen relaxation and phase transition in  $\text{GdBaCo}_2\text{O}_{5+\delta}$  oxide. *Solid State Ionics*, 192, 245–247. doi.org/10.1016/j.ssi.2010.04.028.

[22] J.H. Kim, L. Moggi, F. Prado, A. Caneiro, J.A. Alonso, A. Manthiram. (2009). High temperature crystal chemistry and oxygen permeation properties of the mixed ionic-electronic conductors  $\text{LnBaCo}_2\text{O}_{5+\delta}$  (Ln = Lanthanide). *J. Electrochem. Soc.*, 156, B1376–1382. doi.org/10.1149/1.3231501.

[23] A. Subardi, C. Ching-Cheng, C. Meng-Hsien, C. Wen-Ku, Y.P. Fu. (2016). Electrical, thermal and electrochemical properties of  $\text{SmBa}_{1-x}\text{Sr}_x\text{Co}_2\text{O}_{5+\delta}$  cathode materials for intermediate-temperature solid oxide fuel cells. *Electrochim Acta*, 204, 118–27. 10.1016/j.electacta.2016.04.069.

[24] S. Lu, G. Long, X. Meng, Y. Ji, B. Lu, H. Zhao. (2012).  $\text{PrBa}_{0.5}\text{Sr}_{0.5}\text{Co}_2\text{O}_{5+\delta}$  as cathode material based on LSGM and GDC electrolyte for intermediate-temperature solid oxide fuel cells. *Int. J. Hydrogen Energy*, 37, 5914–5919. doi.org/10.1016/j.ijhydene.2011.12.134.

[25] Y.P. Fu, S.B. Wen, C.H. Lu. (2008). Preparation and characterization of Samaria-doped ceria electrolyte materials for solid oxide fuel cells. *J Am Ceram Soc.*, 91, 127–31. doi.org/10.1111/j.1551-2916.2007.01923.x.

[26] M. Kuhn, J.J. Kim, S.R. Bishop, H.L. Tuller. (2013). Oxygen nonstoichiometry and defect chemistry of perovskite-structured  $\text{Ba}_x\text{Sr}_{1-x}\text{Ti}_{1-y}\text{Fe}_y\text{O}_{3-y/2+\delta}$ . *Chem Mater.*, 25, 2970–75. doi.org/10.1021/cm400546z.

[27] A. Subardi, C. Ching-Cheng, C. Meng-Hsien, C. Wen-Ku, Y.P. Fu. (2016). Electrical, thermal and electrochemical properties of  $\text{SmBa}_{1-x}\text{Sr}_x\text{Co}_2\text{O}_{5+\delta}$  cathode materials for intermediate-temperature solid oxide fuel cells. *Electrochim Acta*, 204, 118–27. 10.1016/j.electacta.2016.04.069.

[28] Y.P. Fu, J. Ouyang, C.H. Li, S.H. Hu. (2013). Chemical bulk diffusion coefficient of  $\text{Sm}_{0.5}\text{Sr}_{0.5}\text{CoO}_{3-\delta}$  cathode for solid oxide fuel cells. *J Power Sources*, 240, 168–77. doi.org/10.1016/j.jpowsour.2013.03.138.

[29] T.V. Aksenova, L.Y. Gavrilova, A.A. Yaremchenko, V.A. Cherepanov, V.V. Kharton. (2012). Oxygen nonstoichiometry, thermal expansion, and high-temperature electrical properties of layered  $\text{NdBaCo}_2\text{O}_{5+\delta}$  and  $\text{SmBaCo}_2\text{O}_{5+\delta}$ . *Mater Res Bull*, 45, 1288–1292. doi.org/10.1016/j.materresbull.2010.05.004.

[30] K. Zhang, L. Ge, R. Ran, Z. Shao, S. Liu. (2008). Synthesis, characterization, and evaluation of cation-ordered  $\text{LnBaCo}_2\text{O}_{5+\delta}$  as materials of oxygen permeation membranes and cathodes of SOFCs. *Acta Mater.*, 56, 4876–4889. doi.org/10.1016/j.actamat.2008.06.004.

[31] K. Jiyoun, C. Sihyuk, P. Seonhye, K. Changmin, S. Jeeyoung, K. Guntae. (2013). Effect of Mn on the electrochemical properties of a layered perovskite  $\text{NdBa}_{0.5}\text{Sr}_{0.5}\text{Co}_{2-x}\text{Mn}_x\text{O}_{5+\delta}$  ( $x = 0, 0.25, \text{ and } 0.5$ ) for intermediate-temperature solid oxide fuel cells. *Electrochim Acta*, 112, 712–718. doi.org/10.1016/j.electacta.2013.09.014.

[32] A. Subardi, Y.P. Fu. (2017). Electrochemical and thermal properties of  $\text{SmBa}_{0.5}\text{Sr}_{0.5}\text{Co}_2\text{O}_{5+\delta}$  cathode impregnated with  $\text{Ce}_{0.8}\text{Sm}_{0.2}\text{O}_{1.90}$  nanoparticles for intermediate temperature solid oxide fuel cells. *Int J Hydrogen Energy*, 42, 24338–24346. doi.org/10.1016/j.ijhydene.2017.08.010.

- [33] M. West, A. Manthiram. (2013). Layered  $\text{LnBa}_{1-x}\text{Sr}_x\text{CoCuO}_{5+\delta}$  (Ln = Nd and Gd) perovskite cathodes for intermediate temperature solid oxide fuel cell. *J Hydrogen Energy*, 38, 3364–72. doi.org/10.1016/j.ijhydene.2012.12.133.
- [34] M.B. Choi, K.T. Lee, H.S. Yoon, S.Y. Jeon, E.D. Wachsman, S.J. Song. (2012). Electrochemical properties of ceria-based intermediate temperature solid oxide fuel cells using microwave heated  $\text{La}_{0.1}\text{Sr}_{0.9}\text{Co}_{0.8}\text{Fe}_{0.2}\text{O}_{3-\delta}$  as a cathode. *J Power Sources*, 220, 377–382. doi.org/10.1016/j.jpowsour.2012.07.122.
- [35] A. Jun, J. Shin, G. Kim. (2013). High redox and performance stability of layered  $\text{SmBa}_{1-x}\text{Sr}_x\text{Co}_{1.5}\text{Cu}_{0.25}\text{O}_{5+\delta}$  perovskite cathodes for intermediate-temperature solid oxide fuel cells. *Phys Chem Phys.*, 15, 19906–19912. doi.org/10.1039/c3cp53883d.
- [36] G.C. Kostogloudis, N. Vasilakos, C. Ftikos. (1998). Crystal structure, thermal and electrical properties of  $\text{Pr}_{1-x}\text{Sr}_x\text{CoO}_{3-\delta}$  ( $x = 0, 0.15, 0.3, 0.4, 0.5$ ) perovskite oxides. *Solid State Ionics*, 106, 207–218. doi.org/10.1016/s0167-2738(97)00506-7.
- [37] P. Meuffels. (2007). Propane gas sensing with high density  $\text{SrTi}_{0.6}\text{Fe}_{0.4}\text{O}_{3-\delta}$  ceramics evaluated by thermogravimetric analysis. *J Eur Ceram Soc.*, 27, 285–290. doi.org/10.1016/j.jeurceramsoc.2006.05.078.
- [38] S. Lia, W. Jin, N. Xu, J. Shi. (2001). Mechanical strength, and oxygen and electronic transport properties of  $\text{SrCo}_{0.4}\text{Fe}_{0.6}\text{O}_{3-\delta}$ -YSZ membranes. *J Membr Sci.*, 186, 195–204. doi.org/10.1016/s0376-7388(00)00681-5.
- [39] G. Kim, S. Wang, A.J. Jacobson, L. Reimus, P. Brodersen, C.A. Mims. (2007). Rapid oxygen ion diffusion and surface exchange kinetics in  $\text{PrBaCo}_2\text{O}_{5+\delta}$  with a perovskite-related structure and ordered A cations. *J Mater Chem.*, 17, 2500–2505. doi.org/10.1039/b618345j.
- [40] M. Fuchang, X. Tian, W. Jingping, S. Zhan, Z. Hui, B. Jean-Marc. (2014). Evaluation of layered perovskites  $\text{YBa}_{1-x}\text{Sr}_x\text{Co}_2\text{O}_{5+\delta}$  as cathodes for intermediate-temperature solid oxide fuel cells. *Int J Hydrogen Energy*, 39, 4531–4543. doi.org/10.1016/j.ijhydene.2014.01.008.
- [41] S.W. Baek, J.H. Kim, J. Bae. (2008). Characteristics of  $\text{ABO}_3$  and  $\text{A}_2\text{BO}_4$  (A = Sm, Sr; B = Co Fe, Ni) samarium oxide system as cathode materials for intermediate temperature-operating solid oxide fuel cell. *Solid State Ionics*, 179, 1570–1574. doi.org/10.1016/j.ssi.2007.12.010.
- [42] J. H. Nam, D.H. Jeon. (2006). A Comprehensive microscale model for transport and reaction in intermediate temperature solid oxide fuel cell. *Electrochim Acta*, 51, 3446–3460. doi.org/10.1016/j.electacta.2005.09.041.
- [43] M. Anderson, J. Yuan, B. Sunden. Review on modeling development for multiscale chemical reactions coupled transport phenomena in the solid oxide fuel cell. *Appl Energy*, 87, 1461–1476. doi.org/10.1016/j.apenergy.2009.11.013.

## References

- [1] B.C.H. Steele, A. Heinzl. (2001). Materials for fuel-cell technologies. *Nature*, 414, 345–352. doi.org/10.1038/35104620.
- [2] N.Q. Minh. (1993). Ceramic fuel cell. *J Am Ceram Soc.*, 76, 563–588. doi.org/10.1111/j.1151-2916.1993.tb03645.x.

- [3] J.C. Ruiz-Molares, D. Marrero-López, J. Canales-Vázquez, J.T.S. Irvine. (2011). Symmetric and reversible solid oxide fuel cells. *RSC Adv.*, 1, 1403–1414. doi.org/10.1039/c1ra00284h.
- [4] S.J. Skinner. (2011). Recent advances in perovskite-type materials for solid oxide fuel cell cathodes. *Int. J. Inorg. Mater.*, 3, 113–121. doi.org/10.1016/s1466-6049(01)00004-6.
- [5] D.J.L. Brett, A. Atkinson, N.P. Brandon, S.J. Skinner. (2008). Intermediate temperature solid oxide fuel cells. *Chem Soc Rev.*, 37, 1568–1578. doi.org/10.1039/b612060c .
- [6] H.Y. Liu, X.F. Zhu, M.J. Cheng, Y. Cong, W.S. Yang. (2011). Novel  $\text{Mn}_{1.5}\text{Co}_{1.5}\text{O}_4$  spinel cathodes for intermediate solid oxide fuel cells. *Chem Commun.*, 47, 2378–2380. doi.org/10.1039/c0cc04300a.
- [7] S.B. Adler. (2004). Factors governing oxygen reduction in solid oxide fuel cell cathodes. *Chem Rev.*, 104, 4791–4844. doi.org/10.1021/cr020724o.
- [8] Y. Takeda, R. Kanno, M. Noda, Y. Tomida, O. Yamamoto. (1987). Cathodic polarization phenomena of perovskite oxide electrodes with stabilized zirconia. *Journal of The Electrochemical Society* volume, 134, 2656–2661. doi.org/10.1149/1.2100267.
- [9] S.B. Adler, J.A. Lane, B.C.H. Steele. (1996). Electrode kinetics of porous mixed-conducting oxygen electrodes. *J Electrochem Soc.*, 143, 3554–3564. doi.org/10.1149/1.1837252.
- [10] A. Subardi, M.H. Cheng, Y.P. Fu. (2014). Chemical bulk diffusion and electrochemical properties of  $\text{SmBa}_{0.6}\text{Sr}_{0.4}\text{Co}_2\text{O}_{5+\delta}$  cathode for intermediate solid oxide fuel cells. *Int J Hydrogen Energy*, 39, 20783–20790. doi.org/10.1016/j.ijhydene.2014.06.134.
- [11] F. Zhao, S. Wang, K. Brinkman, F. Chen. (2010). Layered perovskite  $\text{PrBa}_{0.5}\text{Sr}_{0.5}\text{Co}_2\text{O}_{5+\delta}$  as high performance cathode for solid oxide fuel cells using oxide proton-conducting electrolyte. *J Power Sources*, 195, 5468–5473. doi.org/10.1016/j.jpowsour.2010.03.088.
- [12] Q. Zhou, T. He, Y. Ji. (2008).  $\text{SmBaCo}_2\text{O}_{5+\delta}$  double-perovskite structure cathode material for intermediate-temperature solid-oxide fuel cells. *J Power Sources*, 185, 754–758. doi.org/10.1016/j.jpowsour.2008.07.064.
- [13] A. Tarancon, M. Burriel, J. Santiso, S.J., Skinner, J.A. Kilner. (2010). Advances in layered oxide cathodes for intermediate temperature solid oxide fuel cells. *J Mater Chem.*, 20, 3799–3813. doi.org/10.1039/b922430k.
- [14] D.J. Chen, R. Ran, K. Zhang, J. Wang, Z.P. Shao. (2009). Intermediate-temperature electrochemical performance of a polycrystalline  $\text{PrBaCo}_2\text{O}_{5+\delta}$  cathode on samarium-doped ceria electrolyte. *J Power Sources*, 188, 96–105. doi.org/10.1016/j.jpowsour.2008.11.045.
- [15] C. Kuroda, K. Zheng, K. Swierczek. (2013). Characterization of novel  $\text{GdBa}_{0.5}\text{Sr}_{0.5}\text{Co}_{2-x}\text{FexO}_{5+\delta}$  perovskites for application in IT-SOFC cells. *Int. J. Hydrogen Energy*, 38, 1027–1038. doi.org/10.1016/j.ijhydene.2012.10.085.
- [16] A. Tarancon, A. Morata, G. Dezanneau, S.J. Skinner, J.A. Kilner, A. Estrade, F.H. Ramirez, F. Peiro, J.R. Morante. (2007).  $\text{GdBaCo}_2\text{O}_{5+\delta}$  layered perovskite as an intermediate temperature solid oxide fuel cell cathode. *J. Power*



Sources, 174, 255–263. doi.org/10.1016/j.jpowsour.2007.08.077

[17] A. Chang, S.J. Skinner, J.A. Kilner. (2006). Electrical properties of  $\text{GdBaCo}_2\text{O}_{5+\delta}$  for SOFC applications. *Solid State Ionics*, 177, 2009–2011. doi.org/10.1016/j.ssi.2006.05.047.

[18] H. Gu, H. Chen, L. Gao, Y. Zheng, X. Zhu, L. Guo. (2009). Oxygen reduction mechanism of  $\text{NdBaCo}_2\text{O}_{5+\delta}$  cathode for intermediate-temperature solid oxide fuel cells under cathodic polarization. *Int. J. Hydrogen Energy*, 34, 2416–2420. doi.org/10.1016/j.ijhydene.2009.01.003.

[19] X. Kong, X. Ding. (2011). Novel layered perovskite  $\text{SmBaCu}_2\text{O}_{5+\delta}$  as a potential cathode for intermediate temperature solid oxide fuel cells. *Int. J. Hydrogen Energy*, 36, 15715–15721. doi.org/10.1016/j.ijhydene.2011.09.035.

[20] J.H. Kim, Y. Kim, P.A. Connor, J.T.S. Irvine, J. Bae, W. Zhou. (2009). Structural thermal and electrochemical properties of layered perovskite  $\text{SmBaCo}_2\text{O}_{5+\delta}$ , a potential cathode material for intermediate-temperature solid oxide fuel cells. *J. Power Sources*, 194, 704–711. doi.org/10.1016/j.jpowsour.2009.06.024.

[21] W. Liu, C. Yang, X. Wu, H. Gao, Z. Chen. (2011). Oxygen relaxation and phase transition in  $\text{GdBaCo}_2\text{O}_{5+\delta}$  oxide. *Solid State Ionics*, 192, 245–247. doi.org/10.1016/j.ssi.2010.04.028.

[22] J.H. Kim, L. Moggi, F. Prado, A. Caneiro, J.A. Alonso, A. Manthiram. (2009). High temperature crystal chemistry and oxygen permeation properties of the mixed ionic-electronic conductors  $\text{LnBaCo}_2\text{O}_{5+\delta}$  (Ln = Lanthanide). *J. Electrochem. Soc.*, 156, B1376–1382. doi.org/10.1149/1.3231501.

[23] A. Subardi, C. Ching-Cheng, C. Meng-Hsien, C. Wen-Ku, Y.P. Fu. (2016). Electrical, thermal and electrochemical properties of  $\text{SmBa}_{1-x}\text{Sr}_x\text{Co}_2\text{O}_{5+\delta}$  cathode materials for intermediate-temperature solid oxide fuel cells. *Electrochim Acta*, 204, 118–27. doi.org/10.1016/j.electacta.2016.04.069.

[24] S. Lu, G. Long, X. Meng, Y. Ji, B. Lu, H. Zhao. (2012).  $\text{PrBa}_{0.5}\text{Sr}_{0.5}\text{Co}_2\text{O}_{5+\delta}$  as cathode material based on LSGM and GDC electrolyte for intermediate-temperature solid oxide fuel cells. *Int. J. Hydrogen Energy*, 37, 5914–5919. doi.org/10.1016/j.ijhydene.2011.12.134.

[25] Y.P. Fu, S.B. Wen, C.H. Lu. (2008). Preparation and characterization of Samaria-doped ceria electrolyte materials for solid oxide fuel cells. *J Am Ceram Soc.*, 91, 127–31. doi.org/10.1111/j.1551-2916.2007.01923.x.

[26] M. Kuhn, J.J. Kim, S.R. Bishop, H.L. Tuller. (2013). Oxygen nonstoichiometry and defect chemistry of perovskite-structured  $\text{Ba}_x\text{Sr}_{1-x}\text{Ti}_{1-y}\text{Fe}_y\text{O}_{3-y/2+\delta}$ . *Chem Mater.*, 25, 2970–75. doi.org/10.1021/cm400546z.

[27] A. Subardi, C. Ching-Cheng, C. Meng-Hsien, C. Wen-Ku, Y.P. Fu. (2016). Electrical, thermal and electrochemical properties of  $\text{SmBa}_{1-x}\text{Sr}_x\text{Co}_2\text{O}_{5+\delta}$  cathode materials for intermediate-temperature solid oxide fuel cells. *Electrochim Acta*, 204, 118–27. doi.org/10.1016/j.electacta.2016.04.069.

[28] Y.P. Fu, J. Ouyang, C.H. Li, S.H. Hu. (2013). Chemical bulk diffusion coefficient of  $\text{Sm}_{0.5}\text{Sr}_{0.5}\text{CoO}_{3-\delta}$  cathode for solid oxide fuel cells. *J Power Sources*, 240, 168–77. doi.org/10.1016/j.jpowsour.2013.03.138.

[29] T.V. Aksenova, L.Y. Gavrilova, A.A. Yaremchenko, V.A. Cherepanov, V.V. Kharton. (2012). Oxygen nonstoichiometry, thermal expansion, and high-

temperature electrical properties of layered  $\text{NdBaCo}_2\text{O}_{5+\delta}$  and  $\text{SmBaCo}_2\text{O}_{5+\delta}$ . *Mater Res Bull*, 45, 1288–1292. doi.org/10.1016/j.materresbull.2010.05.004.

[30] K. Zhang, L. Ge, R. Ran, Z. Shao, S. Liu. (2008). Synthesis, characterization, and evaluation of cation-ordered  $\text{LnBaCo}_2\text{O}_{5+\delta}$  as materials of oxygen permeation membranes and cathodes of SOFCs. *Acta Mater.*, 56, 4876–4889. doi.org/10.1016/j.actamat.2008.06.004.

[31] K. Jiyoun, C. Sihyuk, P. Seonhye, K. Changmin, S. Jeeyoung, K. Guntae. (2013). Effect of Mn on the electrochemical properties of a layered perovskite  $\text{NdBa}_{0.5}\text{Sr}_{0.5}\text{Co}_{2-x}\text{Mn}_x\text{O}_{5+\delta}$  ( $x = 0, 0.25, \text{ and } 0.5$ ) for intermediate-temperature solid oxide fuel cells. *Electrochim Acta*, 112, 712–718. doi.org/10.1016/j.electacta.2013.09.014.

[32] A. Subardi, Y.P. Fu. (2017). Electrochemical and thermal properties of  $\text{SmBa}_{0.5}\text{Sr}_{0.5}\text{Co}_2\text{O}_{5+\delta}$  cathode impregnated with  $\text{Ce}_{0.8}\text{Sm}_{0.2}\text{O}_{1.90}$  nanoparticles for intermediate temperature solid oxide fuel cells. *Int J Hydrogen Energy*, 42, 24338–24346. doi.org/10.1016/j.ijhydene.2017.08.010.

[33] M. West, A. Manthiram. (2013). Layered  $\text{LnBa}_{1-x}\text{Sr}_x\text{CoCuO}_{5+\delta}$  ( $\text{Ln} = \text{Nd and Gd}$ ) perovskite cathodes for intermediate temperature solid oxide fuel cell *Int. J Hydrogen Energy*, 38, 3364–72. doi.org/10.1016/j.ijhydene.2012.12.133.

[34] M.B. Choi, K.T. Lee, H.S. Yoon, S.Y. Jeon, E.D. Wachsman, S.J. Song. (2012). Electrochemical properties of ceria-based intermediate temperature solid oxide fuel cells using microwave heated  $\text{La}_{0.1}\text{Sr}_{0.9}\text{Co}_{0.8}\text{Fe}_{0.2}\text{O}_{3-\delta}$  as a cathode. *J Power Sources*, 220, 377–382. doi.org/10.1016/j.jpowsour.2012.07.122.

[35] A. Jun, J. Shin, G. Kim. (2013). High redox and performance stability of layered  $\text{SmBa}_{1-x}\text{Sr}_x\text{Co}_{1.5}\text{Cu}_{0.25}\text{O}_{5+\delta}$  perovskite cathodes for intermediate-temperature solid oxide fuel cells. *Phys Chem Phys.*, 15, 19906–19912. doi.org/10.1039/c3cp53883d.

[36] G.C. Kostogloudis, N. Vasilakos, C. Ftikos. (1998). Crystal structure, thermal and electrical properties of  $\text{Pr}_{1-x}\text{Sr}_x\text{CoO}_{3-\delta}$  ( $x = 0, 0.15, 0.3, 0.4, 0.5$ ) perovskite oxides. *Solid State Ionics*, 106, 207–218. doi.org/10.1016/s0167-2738(97)00506-7.

[37] P. Meuffels. (2007). Propane gas sensing with high density  $\text{SrTi}_{0.6}\text{Fe}_{0.4}\text{O}_{3-\delta}$  ceramics evaluated by thermogravimetric analysis. *J Eur Ceram Soc.*, 27, 285–290. doi.org/10.1016/j.jeurceramsoc.2006.05.078.

[38] S. Lia, W. Jin, N. Xu, J. Shi. (2001). Mechanical strength, and oxygen and electronic transport properties of  $\text{SrCo}_{0.4}\text{Fe}_{0.6}\text{O}_{3-\delta}$ -YSZ membranes. *J Membr Sci.*, 186, 195–204. doi.org/10.1016/s0376-7388(00)00681-5.

[39] G. Kim, S. Wang, A.J. Jacobson, L. Reimus, P. Brodersen, C.A. Mims. (2007). Rapid oxygen ion diffusion and surface exchange kinetics in  $\text{PrBaCo}_2\text{O}_{5+\delta}$  with a perovskite-related structure and ordered A cations. *J Mater Chem.*, 17, 2500–2505. doi.org/10.1039/b618345j.

[40] M. Fuchang, X. Tian, W. Jingping, S. Zhan, Z. Hui, B. Jean-Marc. (2014). Evaluation of layered perovskites  $\text{YBa}_{1-x}\text{Sr}_x\text{Co}_2\text{O}_{5+\delta}$  as cathodes for intermediate-temperature solid oxide fuel cells. *Int J Hydrogen Energy*, 39, 4531–4543. doi.org/10.1016/j.ijhydene.2014.01.008.

[41] S.W. Baek, J.H. Kim, J. Bae. (2008). Characteristics of  $\text{ABO}_3$  and

A<sub>2</sub>B<sub>4</sub>O<sub>4</sub> (A = Sm, Sr; B = Co, Fe, Ni) samarium oxide system as cathode materials for intermediate temperature-operating solid oxide fuel cell. *Solid State Ionics*, 179, 1570–1574. doi.org/10.1016/j.ssi.2007.12.010.

[42] J. H. Nam, D.H. Jeon. (2006). A Comprehensive microscale model for transport and reaction in intermediate temperature solid oxide fuel cell. *Electrochim Acta*, 51, 3446–3460. doi.org/10.1016/j.electacta.2005.09.041.

[43] M. Anderson, J. Yuan, B. Sunden. Review on modeling development for multiscale chemical reactions coupled transport phenomena in the solid oxide fuel cell. *Appl Energy*, 87, 1461–1476. doi.org/10.1016/j.apenergy.2009.11.013.

Adi Subardi

Doctor of Materials Science and Engineering, Assistance Professor

Department of Mechanical Engineering

Institut Teknologi Nasional Yogyakarta

Jl Babarsari Caturtunggal, Depok, Sleman, Daerah Istimewa Yogyakarta, Indonesia, 55281

E-mail: subardi@itny.ac.id

Contact phone: +6282133167082

The number of articles in international databases: 9

H-index: 4

ORCID: <https://orcid.org/0000-0003-0867-3624>

[https://www.researchgate.net/profile/Adi\\_Subardi](https://www.researchgate.net/profile/Adi_Subardi)

[https://scholar.google.com/scholar?hl=id&as\\_sdt=0%2C5&q=adi+subardi&btnG](https://scholar.google.com/scholar?hl=id&as_sdt=0%2C5&q=adi+subardi&btnG)

Iwan Susanto

Doctor of Materials Science and Engineering, Assistance Professor

Department of Mechanical Engineering

Politeknik Negeri Jakarta

Jl. Prof. DR. G.A. Siwabessy, Kukusan, Kecamatan Beji, Kota Depok, Jawa Barat, Indonesia, 16424

E-mail: iwan.susanto@mesin.pnj.ac.id

Contact phone: +6281932421764, +62217863530

The number of articles in international databases: 5

H-index: 2

ORCID: <http://orcid.org/0000-0001-7120-0374>

[https://www.researchgate.net/profile/Iwan\\_Susanto3](https://www.researchgate.net/profile/Iwan_Susanto3)

Ratna Kartikasari

Doctor of Mechanical Engineering, Associate Professor

Department of Mechanical Engineering

Institut Teknologi Nasional Yogyakarta

Jl Babarsari Caturtunggal, Depok, Sleman, Daerah Istimewa Yogyakarta, Indonesia, 55281

E-mail: ratna@itny.ac.id

Contact phone: +6281392019208

The number of articles in international databases: 4

H-index: 2

ORCID: <https://orcid.org/0000-0001-8859-3258>

[https://www.researchgate.net/profile/Ratna\\_Kartikasari](https://www.researchgate.net/profile/Ratna_Kartikasari)

[https://scholar.google.com/scholar?hl=id&as\\_sdt=0%2C5&q=ratna+kartikasari&oq=Ratna+Kartika](https://scholar.google.com/scholar?hl=id&as_sdt=0%2C5&q=ratna+kartikasari&oq=Ratna+Kartika)

Tugino Tugino

Master of Electrical Engineering, Associate Professor

Department of Electrical Engineering

Institut Teknologi Nasional Yogyakarta

Jl Babarsari Caturtunggal, Depok, Sleman, Daerah Istimewa Yogyakarta, Indonesia, 55281

E-mail: [tugino@itny.ac.id](mailto:tugino@itny.ac.id)

Contact phone: +62 81578873090

The number of articles in international databases: -

H-index: -

ORCID: <https://orcid.org/0000-0003-0297-088X>

Hasta Kuntara

Master of Mechanical Engineering, Assistance Professor

Department of Mechanical Engineering

Institut Teknologi Nasional Yogyakarta

Jl Babarsari Caturtunggal, Depok, Sleman, Daerah Istimewa Yogyakarta, Indonesia, 55281

E-mail: [hasta@itny.ac.id](mailto:hasta@itny.ac.id)

Contact phone: + 6285728856654

The number of articles in international databases: -

H-index: -

ORCID: <https://orcid.org/0000-0002-3518-0692>

Andy Erwin Wijaya

Doctor of Mining Engineering, Assistance Professor

Department of Mining Engineering,

Institut Teknologi Nasional Yogyakarta

Jl Babarsari Caturtunggal, Depok, Sleman, Daerah Istimewa Yogyakarta, Indonesia, 55281

E-mail: [andyerwin@itny.ac.id](mailto:andyerwin@itny.ac.id)

Contact phone: +6282300182053

The number of articles in international databases: -

H-index: -

ORCID: <https://orcid.org/0000-0002-3613-3935>

[https://scholar.google.com/scholar?hl=id&as\\_sdt=0%2C5&q=andy+erwin+wijaya&btnG=](https://scholar.google.com/scholar?hl=id&as_sdt=0%2C5&q=andy+erwin+wijaya&btnG=)

Ade Indra

Doctor Cand. (Ph.D.), Associate professor

Department of Mechanical Engineering

Institut Teknologi Padang (ITP)

Jl. Gajah Mada Jl. Kandis Raya, Kp. Olo, Kec. Nanggalo, Kota Padang, West Sumatera Barat, Indonesia, 25173

E-mail: [adeindra@itp.ac.id](mailto:adeindra@itp.ac.id)

Contact phone: +6281363243101

The number of articles in international databases: 2

H-index: 1

ORCID: <https://orcid.org/0000-0003-3048-4758>

<https://www.researchgate.net/scientific-contributions/Ade-Indra-2120638266>

Hendriwan Fahmi

Master of Mechanical Engineering, Associate Professor

Department of Mechanical Engineering

Institut Teknologi Padang (ITP)

Jl. Gajah Mada Jl. Kandis Raya, Kp. Olo, Kec. Nanggalo, Kota Padang, West Sumatera Barat, Indonesia, 25173

E-mail: [hendriwan\\_f@yahoo.com](mailto:hendriwan_f@yahoo.com)

Contact phone: +6281363265251

The number of articles in international databases: 4

H-index: 2

ORCID: <https://orcid.org/0000-0002-8129-4316>

[https://www.researchgate.net/profile/Hendriwan\\_Fahmi](https://www.researchgate.net/profile/Hendriwan_Fahmi)

Yen-Pei Fu

Doctor of Materials, Professor

Department of Materials Science and Engineering

National Dong Hwa University

Shoufeng Township, Hualien, Taiwan ROC, 97401

E-mail: [ypfu@mail.ndhu.edu.tw](mailto:ypfu@mail.ndhu.edu.tw)

Contact phone: + 886-3-8634212

The number of articles in international databases: 147

H-index: 24

ORCID: <https://orcid.org/0000-0002-2472-4981>

[https://www.researchgate.net/profile/Yen-Pei\\_Fu](https://www.researchgate.net/profile/Yen-Pei_Fu)

[researchgate.net/profile/Yen-Pei\\_Fu](https://www.researchgate.net/profile/Yen-Pei_Fu)

Filing Date: 16.12.2020

Adoption Date:

**UDC 539**

## **ANALYSIS OF $\text{SmBa}_{0.5}\text{Sr}_{0.5}\text{Co}_2\text{O}_{5+\delta}$ DOUBLE PEROVSKITE OXIDE FOR INTERMEDIATE-TEMPERATURE SOLID OXIDE FUEL CELLS**

**Adi Subardi, Iwan Susanto, Ratna Kartikasari, Tugino Tugino, Hasta Kuntara, Andy Erwin Wijaya, Muh Amin, Muhamad Jalu Purnomo, Ade Indra, Hendriwan Fahmi, Yen-Pei Fu**

**Adi Subardi, Iwan Susanto, Ratna Kartikasari, Tugino Tugino, Hasta Kuntara, Andy Erwin Wijaya, Ade Indra, Hendriwan Fahmi, Yen-Pei Fu**

*The main obstacle to solid oxide fuel cells (SOFCs) implementation is the high operating temperature in the range of 800–1000 °C so that it has an impact on high costs. SOFC working at high temperatures causing rapid breakdown between layers (anode, electrolyte, and cathode) because it has a different thermal expansion. The study focused on reducing the operating temperature in the medium temperature range.  $\text{SmBa}_{0.5}\text{Sr}_{0.5}\text{Co}_2\text{O}_{5+\delta}$  (SBSC) oxide was studied as a cathode material for IT-SOFCs base on  $\text{Ce}_{0.8}\text{Sm}_{0.2}\text{O}_{1.9}$  (SDC) electrolyte. The SBSC powder was prepared using the solid-state reaction method with repeated ball-milling and calcining. Alumina grinding balls are used because they have a high hardness to crush and smooth the powder of SOFC material. The specimens were then tested as cathode material for SOFC at intermediate temperature (600–800 °C) using X-ray powder diffraction (XRD), thermogravimetric analysis (TGA), electrochemical, and Scanning electron microscopy (SEM) tests. The X-ray powder diffraction (XRD) pattern of SBSC powder can be indexed to a tetragonal space group (P4/mmm). The overall change in mass of the SBSC powder is 8 % at a temperature range of 125–800 °C. A sample of SBSC powder showed a high oxygen content ( $5+\delta$ ) that reached 5.92 and 5.41 at temperatures of 200 °C and 800 °C, respectively. High diffusion levels and increased surface activity of oxygen reduction reactions (ORRs) can be affected by high oxygen content ( $5+\delta$ ). The polarization resistance ( $R_p$ ) of samples sintered at 1000 °C is  $4.02 \Omega\text{cm}^2$  at 600 °C,  $1.04 \Omega\text{cm}^2$  at 700 °C, and  $0.42 \Omega\text{cm}^2$  at 800 °C. The power density of the SBSC cathode is 336.1, 387.3, and 357.4  $\text{mW}/\text{cm}^2$  at temperatures of 625 °C, 650 °C, and 675 °C, respectively. The SBSC demonstrates as a prospective cathode material for IT-SOFC*

*Keywords: Solid oxide fuel cell; Thermal properties; Oxygen content; Electrochemical properties; Cell performance*

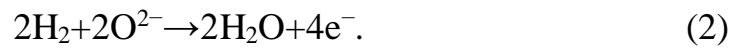
### **1. Introduction**

Limited fossil fuels and global warming are increasingly threatening human survival and have been serious global issues for decades. New power plants using

fuel sources such as solid oxide fuel cells (SOFCs) have attracted much attention around the world, and the technology is expected to reduce obstacles in the supply of electricity in the future. The advantage of SOFCs compared with other types of fuel cells is that they are a more efficient and flexible fuel source. SOFCs also offer low pollutant emissions because the final stage of their usage only produces a vapor or hot water [1–3]. The schematic diagram exhibiting the basic operation of SOFC is shown in Fig. 1, *a*. At the cathode side, the oxygen reduction reaction occurs by accepting electrons from the external circuit. The reactions can be written below:



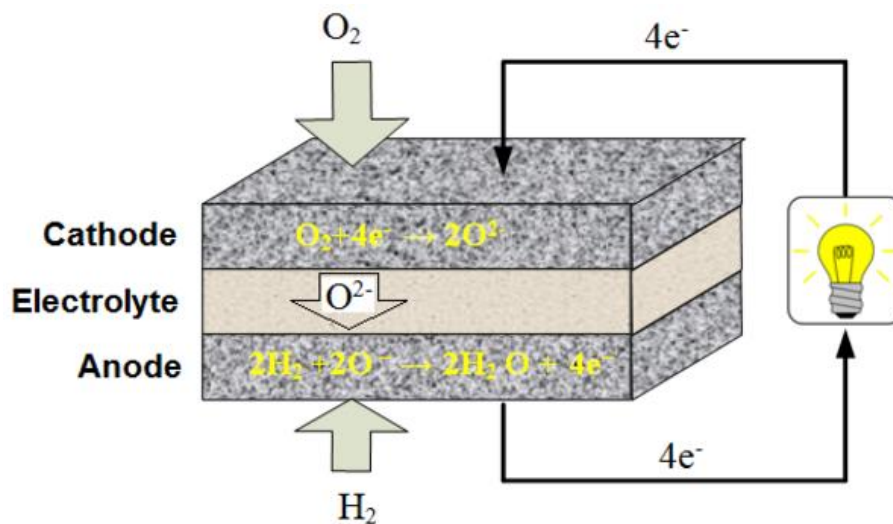
The produced oxide ions ( $\text{O}^{2-}$ ) pass through the electrolyte to the anode side and combine with the protons produced by the oxidation of hydrogen or other fuels to produce water. The reactions can be written:



Overall reaction,



This reaction occurs at the three-phase boundary (TPB) [4]. The TPB is the interfacial area among electrode, electrolyte, and gaseous fuel where the overall reaction occurs (Fig. 1, *b*). The electrons flowing from the anode to the cathode produce electrical work in the “Load”.



*a*



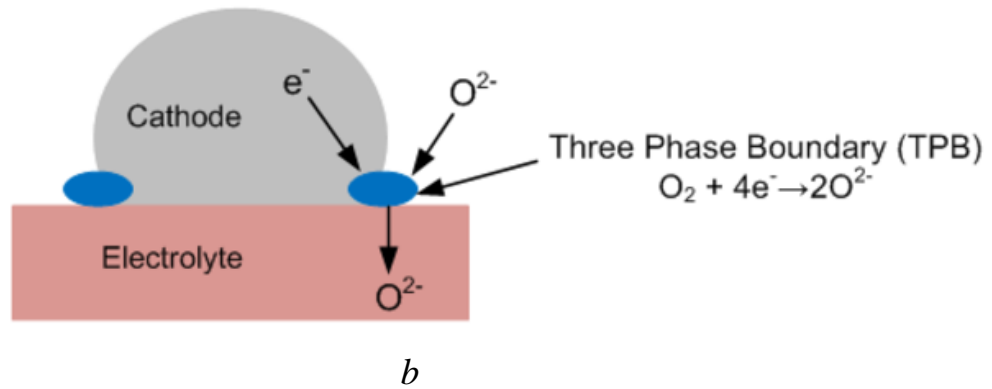


Fig. 1. Schematic diagram: *a* – The SOFC operation; *b* – three-phase boundary (TPB)

Fig. 1. Illustration diagram: *a* – The SOFC operation; *b* – three-phase boundary (TPB)

The Figure is of poor quality. Has been revised

The fonts used in figures should match the font Times New Roman 14.

To improve the quality open the original file of figure (xls for Excel, dwg for AutoCAD, cdr for CorelDRAW etc) and print your figure to pdf (use File->Print of [ctrl]+[P] for it). Then resave pdf to tiff using Photoshop or another editor (be sure that resolution at least 300 dpi). Send me this file.

Through the process, chemical energy is directly converted to electrical energy. To increase the active area where the oxygen reduction reaction (cathode) or hydrogen oxidation reaction (anode) occurs, a porous electrode structure is employed. Meanwhile, the dense electrolyte provides a physical barrier to prevent the direct mixing of fuel and air.

## 2. Literature review and problem statement

In general, traditional SOFCs operate at high temperatures, which causes several problems including high production costs, mismatches in thermal expansion between the fuel cell components, and chemical compatibility. Therefore, current research is focused on SOFCs that can operate at lower temperatures (400–800 °C) and aims to reduce production costs and achieve a long working lifetime (40,000 h) [5–7]. Lower operating temperatures cause the catalytic activity of the electrodes to decrease significantly, and the cathode is a limiting factor for overall fuel cell performance. Therefore, the focus is being directed toward maintaining stability in the cathode material and increasing the high electrochemical performance of IT-SOFCs. In other words, a vital result of the research into fuel cell performance is the discovery that the cathode polarization can be eliminated [8]. However, the application of SOFC is

widely constrained due to the impact of low catalytic activity on the oxygen reduction reactions (ORRs) at the cathode. Mixed ionic-electronic conductor cathodes (MIECs) are successful in increasing the active ORR zone from the three-phase boundary to the cathode-gas interface site, which will reduce cathodic resistance [8, 9]. The ORR site of MIECs works on the TPB (the electrolytes, cathodes, and gas phases) and at the two-phase boundary between the gas phase and the cathode [10].

Recently, among the various MIECs oxides, cobalt-containing perovskite oxides such as  $\text{SmBa}_{0.6}\text{Sr}_{0.4}\text{Co}_2\text{O}_{5+\delta}$  [11],  $\text{PrBa}_{0.5}\text{Sr}_{0.5}\text{Co}_{2-x}\text{Fe}_x\text{O}_{5+\delta}$  [12],  $\text{NdBa}_{1-x}\text{Sr}_x\text{Co}_2\text{O}_{5+\delta}$  [13],  $\text{YBa}_{0.6}\text{Sr}_{0.4}\text{Co}_2\text{O}_{5+\delta}$  [14], and  $\text{GdBa}_{0.5}\text{Sr}_{0.5}\text{Co}_{2-x}\text{Fe}_x\text{O}_{5+\delta}$  [15] have attracted strong interest due to their electrocatalytic activity performance for the ORR. Also, the investigation has been conducted for layered perovskites with the chemical formula  $\text{LnBaCo}_2\text{O}_{5+\delta}$  (Ln-selected lanthanides) [16–23]. Several research groups also have investigated the electrochemical properties of a new type of MIEC oxide, cation ordered  $\text{LnBaCo}_2\text{O}_{5+\delta}$  (Ln=La, Pr, Sm, Gd, Y), as a potential cathode material for IT-SOFCs. Cobalt in cathodes is beneficial for the activation of oxygen reduction and thus provides a lower activation polarization loss. Cobalt-based cathodes, however, have high thermal expansion coefficients (TECs) because of the low-spin to the high-spin transition of Co. The incompatibility in thermal expansion can cause thermal stress in SOFCs and thus result in poor long-term thermal stability [13]. Therefore, it is important to improve the thermal expansion compatibility between the cathodes and the electrolytes. Zhou *et al.* [24] have declared that  $\text{LnBaCo}_2\text{O}_{5+\delta}$  cathodes with an intermediate lanthanide-ion radius, such as  $\text{Sm}^{3+}$ , may provide a compromise between the values of the catalytic activity and thermal expansion coefficients. Recent reports exhibit when A' site is partially substituted by Sr, it could potentially improve the conductivity of double perovskite oxides where Sr-doped oxide  $\text{YBa}_{0.5}\text{Sr}_{0.5}\text{Co}_2\text{O}_{5+\delta}$  demonstrated excellent conductivity values (about 32 times higher than that of the Sr-free sample). Moreover, the Sr-doped layered perovskite oxide system  $\text{LnBa}_{0.5}\text{Sr}_{0.5}\text{Co}_2\text{O}_{5+x}$  (Ln=Pr, Sm, and Gd), which showed a lower polarization resistance based on doped ceria electrolyte [25]. However, observations of SOFC performance in the range of 625, 650, and 675 °C have not been experimentally investigated. From the research reported above, some of the obstacles that SOFC faced were high working temperatures and high thermal expansion differences in SOFC components. Efforts were made to overcome this problem, the use of SBSC material as a cathode is expected to reduce the working temperature of SOFC so that the compatibility of SOFC components meets the requirements. In this work, SBSC oxide is synthesized, and aspects of its structural characteristics, thermal and electrochemical performance, power density, and microstructure are investigated. The SBSC oxygen reduction mechanism is also observed under various oxygen partial pressures (OPPs).

### **3. The aim and objectives of the study**

The aim of this study was to analyze the performance of double perovskite oxides used in intermediate-temperature solid oxide fuel cells.

To achieve this aim, the following objectives are accomplished:

- modify the structure of SBSC cathode by the solid-state reaction method;

- investigate the polarization resistance ( $R_p$ ) of SBSC cathode and the maximum power density obtained in the single cells SOFC;
- performance test of SBSC cathodes at intermediate operating temperatures

#### 4. Materials and methods for preparing and testing specimens

Fig. 2 shows the procedure of preparation for single cell specimen which is composited from three elements SOFC namely anode, electrolyte and cathode materials. The synthesis methods for the cathodes and electrolytes are described in previously published papers [11, 26]. The SBSC cathode powder was prepared using a solid-state reaction technique. The stoichiometric amounts of cathode material ( $\text{Sm}_2\text{O}_3$ ,  $\text{BaCO}_3$ ,  $\text{SrCO}_3$ , and  $\text{CoO}$ ) were ball-milled in ethanol for 12 h. The slurry was then heated at a temperature of  $1000\text{ }^\circ\text{C}$  in the air for 6 h. The  $\text{Ce}_{0.8}\text{Sm}_{0.2}\text{O}$  (SDC) powder was synthesized using the coprecipitation technique using the precursor materials  $\text{Ce}(\text{NO}_3)_3 \cdot 6\text{H}_2\text{O}$  and  $\text{Sm}(\text{NO}_3)_3 \cdot 6\text{H}_2\text{O}$ . A stoichiometric ratio applied, distilled water was then used to dissolve the starting material before being added to the ammonia solution.

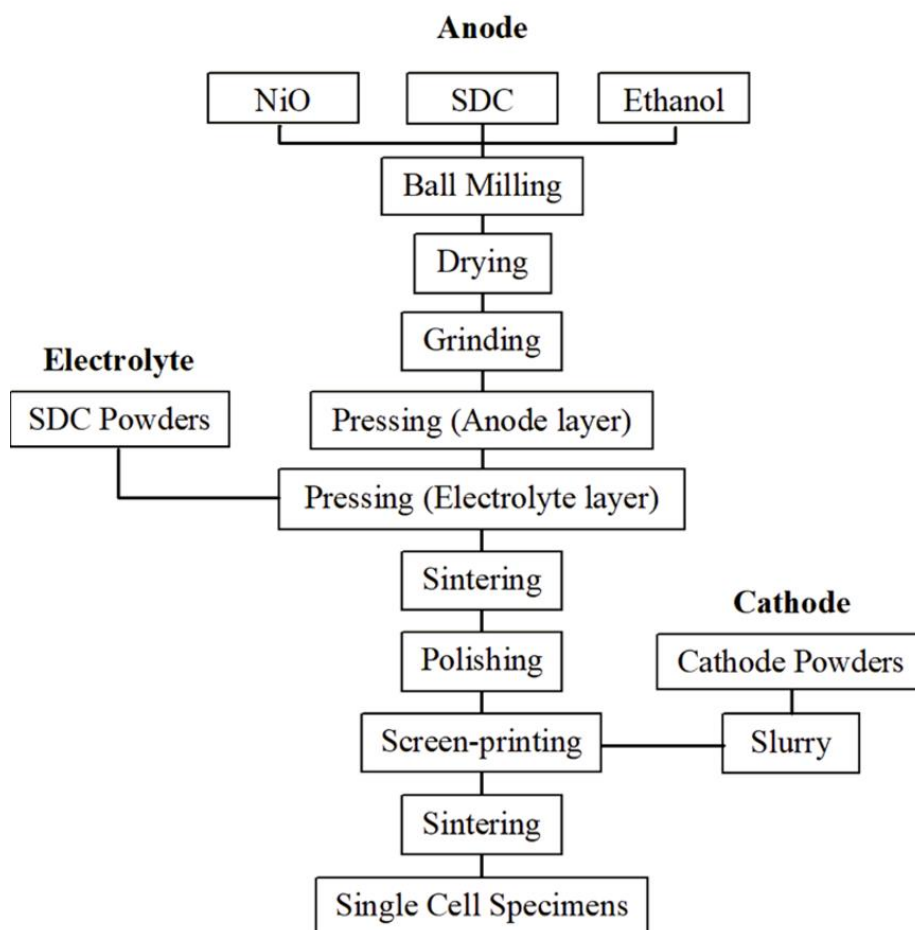


Fig. 2. The procedure of preparation for single-cell specimens

Fig.2. The fabrication procedure for single-cell specimens

The Figure is of poor quality. Has been revised

The pH value ranging from 9.5 to 10 is applied to the mixed solution. The precipitate was washed three times after it was filtered using distilled water and ethanol. In the next process, the co-precipitation powder was heated at 600 °C and held in the air for 2 h. For a binding agent, a small amount of polyvinyl alcohol (PVA) by a purity grade of 96 % was mixed into the SDC powder and then pelletized to dimensions of 1.5 cm in diameter and 0.1 cm in thickness using uniaxial pressure applied at 1000 kg f/cm<sup>2</sup>. The disk-shaped sample was heated at 1500 °C and held for 5 h, followed by cooling to room temperature [26]. The procedure stages of fabricating a single cell specimen, as presented in Fig. 2. The structure of the SBSC cathode powder was observed by XRD using a Rigaku D/MAX-2500V, the radiation source of a Cu K $\alpha$  (1.5418 Å), and a scanning range of 10°–80°. To explain the lattice parameter and powder pattern for the sample, we used the GSAS program to perform a Rietveld refinement. The SBSC cathode microstructure (top view) and the cross-sectional image of the symmetrical cell were investigated by SEM (a Hitachi 3400N). The TG/DTA 6300 was used to analyze the thermo-gravimetric behavior of SBSC cathodes in the air (100 cm<sup>3</sup>/min). The oxygen content was calculated using the following formula:

$$\delta = \frac{M_s \Delta m}{M_o m} \quad (4)$$

The abbreviations/symbols in the formula are explained as follows, the specimen molar mass ( $M_s$ ), the specimen mass in the air at room temperature ( $m$ ), and the molar mass of oxygen ( $M_o$ ) [27]. The cathode paste of SBSC involves cathode powder, the binding agent, a plasticizer, and a solvent, all of which were conducted by ball-mill processes. Screen printing technique was used to prepare a half cell sample of SBSC|SDC|SBSC. The manufacturing details of the half-cell sample are discussed in an earlier paper. The symmetrical cell testing was carried out under air in temperatures ranging from 600 °C to 800 °C in a furnace. The AC impedance measurement was performed using the VoltaLab PGZ301 potentiostat with a frequency applied range from 100 kHz to 0.1 Hz with 10 mV AC signal amplitude. The EIS fitting analysis was performed with the Z-view software [24]. The digital source meter (Keithley 2420) was used to collect Voltage (V) – current (I) from a single cell in the temperature range between 625 °C and 675 °C. Button cells were measured with humidified hydrogen (3 vol % H<sub>2</sub>O) as the fuel and air as the oxidant. The configuration of the single-cell sample was Ni-SDC|SDC|SBSC with a 1.3 cm diameter. In a preceding paper [28], the detailed stages for preparing a single cell are given.

## 5. Result of SBSC Performance Test

### 5.1. Structure of Crystal

The crystal structure and phase composition of the SBSC powder were observed using X-ray diffraction (XRD). From software GSAS analysis, characteristic XRD peaks were detected as double perovskite oxide. The peaks caused by impurities are

not detected in the structure of SBSC, which indicates a well-prepared sample. Meanwhile, the lattice parameters are obtained:  $a=3,861 \text{ \AA}$ ,  $b=3,861 \text{ \AA}$ ,  $c=7,617 \text{ \AA}$ , and  $v=113.56 \text{ \AA}^3$ , with reliability factors of  $R_{wp}=0.41$  and  $R_p=0.23$ . In this structure, Sm atoms are in position 1a, Sr, and Ba atoms are randomly distributed at position 1b. The cell parameters regarding the SBSC cathode structure collected from Rietveld refinement are described in Table 1.

Table 1

Crystallographic data at room temperature for SBSC. Cell parameters were collected using a Rietveld refinement

Atom	Wyckoff position	$x$	$y$	$z$	Uiso	Occ
Sm	1a (0 0 0)	0	0	0	0.0333	0.8797
Co	2h ( $\frac{1}{2} \frac{1}{2} z$ )	$\frac{1}{2}$	$\frac{1}{2}$	0.25592	0.0045	0.9944
Ba/Sr	1b (0 0 $\frac{1}{2}$ )	0	0	$\frac{1}{2}$	0.0092	0.8926
O1	4i (0 $\frac{1}{2} z$ )	0	$\frac{1}{2}$	0.26780	0.0077	0.9311
O2	1c ( $\frac{1}{2} \frac{1}{2} 0$ )	$\frac{1}{2}$	$\frac{1}{2}$	0	0.1906	1.2455
O3	2h ( $\frac{1}{2} \frac{1}{2} z$ )	$\frac{1}{2}$	$\frac{1}{2}$	0.44110	0.0333	0.4220

Meanwhile, the Co atom occupies position 2h (0.5, 0.5,  $z$ ). The SBSC structure has three kinds of oxygen atom sites: O3 at 2h (0.5, 0.5,  $z$ ), O2 at 1c (0.5,0.5,0), and O1 at 4i (0, 0.5,  $z$ ).

Fig. 3 shows the refinement of SBSC patterns including the measured XRD data, the calculated profile, and the difference between them. The refinement using the General Structure Analysis System (GSAS) program is typically used for crystallographic analysis, quantitative phase determination, texture mapping, stress-strain measurements, and other related types of materials characterization. The test results agree with the measured profiles, indicating that in the perovskite lattice, cations are well ordered.

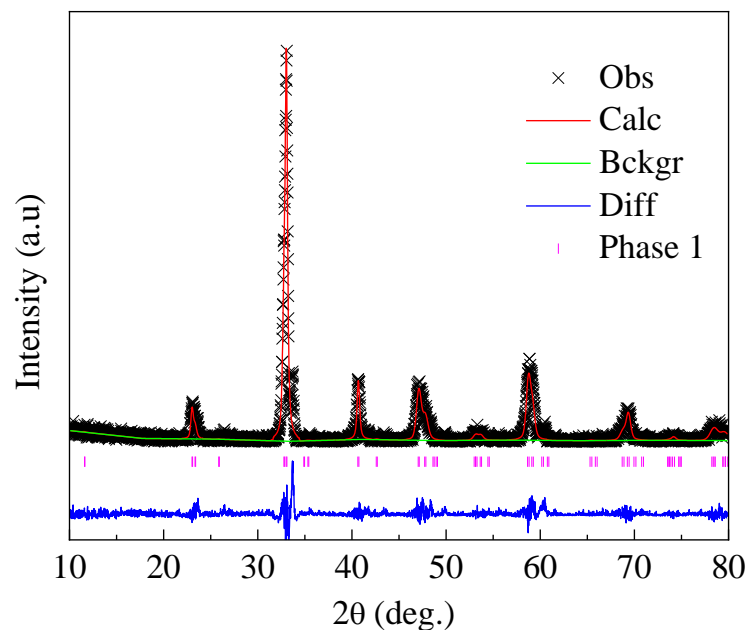


Fig. 3. Rietveld refinement data of the SBSC cathode at room temperature

The space group, fractional coordinates, and lattice parameters of corresponding double perovskite structure cathodes are shown in Table 2.

Table 2

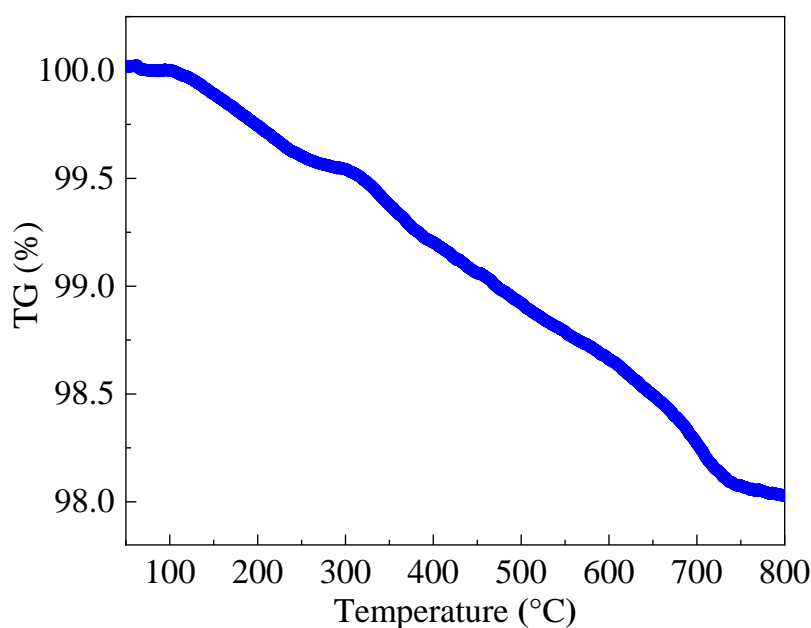
Space group, fractional coordinates, and lattice parameters of corresponding double perovskite structure cathodes

Specimens	Space group	$a(\text{Å})$	$b(\text{Å})$	$c(\text{Å})$	$V(\text{Å}^3)$	$R_{wp}$
NdBaCo <sub>2</sub> O <sub>5+δ</sub> [29]	P4/mmm	3.903	3.903	7.614	116.02	0.42
SmBaCoO <sub>5+δ</sub> [29]	Pmmm	3.886	7.833	7.560	230.22	0.45
NdBa <sub>0.5</sub> Sr <sub>0.5</sub> Co <sub>2</sub> O <sub>5+δ</sub> [30]	P4/mmm	3.861	3.861	7.715	115.01	0.36
NdBa <sub>0.5</sub> Sr <sub>0.5</sub> Co <sub>1.5</sub> Mn <sub>0.5</sub> O <sub>5+δ</sub> [31]	P4/mmm	3.855	3.855	7.705	114.54	0.12
SmBa <sub>0.6</sub> Sr <sub>0.4</sub> Co <sub>2</sub> O <sub>5+δ</sub> [11]	P4/mmm	3.870	3.870	7.590	114.11	0.29
SmBa <sub>0.5</sub> Sr <sub>0.5</sub> Co <sub>2</sub> O <sub>5+δ</sub> [32]	P4/mmm	3.883	3.883	7.580	114.30	0.28

The SBSC cathode showed high structural stability when the samples were calcined under temperatures of 1000 °C and 1200 °C, which does not influence the crystal's structure [33].

## 5. 2. Thermal properties and oxygen content analysis

To clarify the oxygen content of the SBSC cathode, TGA was conducted in the air. The TGA curve indicates that the specimen had slight weight loss before 125 °C, which is associated with the desorption of the specimen's absorbed water as presented in Fig. 4, *a*. With a further increase in temperature, the magnitude of weight loss became significant and continued until weight loss slowed at temperatures of 250–325 °C.



*a*

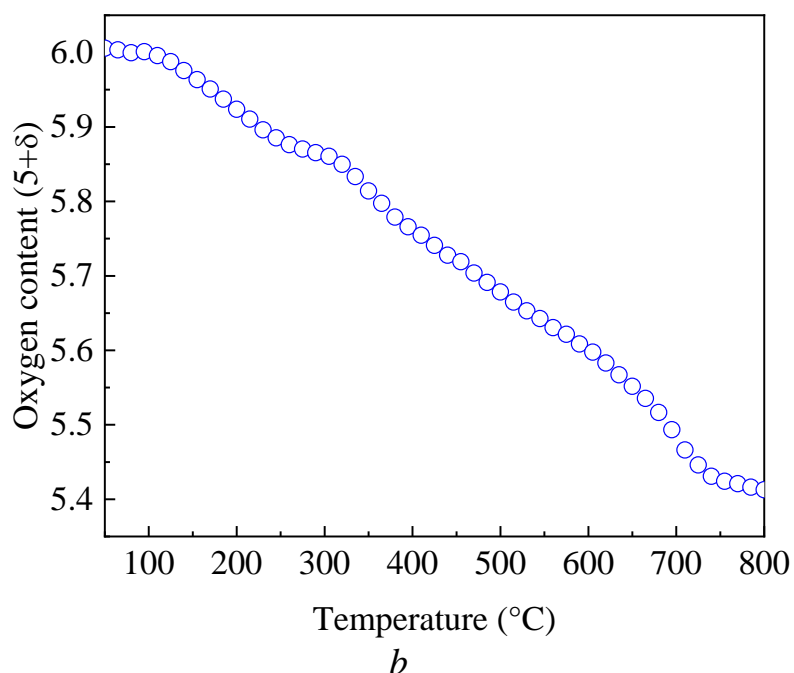


Fig. 4. The Curve data: *a* – The TGA of the SBSC powder over a temperature range between 27 °C and 800 °C; *b* – the oxygen content (5+δ) as a function of temperature in air for SBSC cathodes

Above 325 °C, the rate of degradation in weight loss was significant, and the mass change slowed again at temperatures around 725 °C. It can be seen that from 650 °C to 750 °C the weight loss rate tends to increase. Then, at a temperature range of 750 °C, weight loss seems to slow down again until it reaches a temperature of 800 °C. Detailed oxygen content (5+δ) information as a function of temperature is listed in Table 3.

Table 3

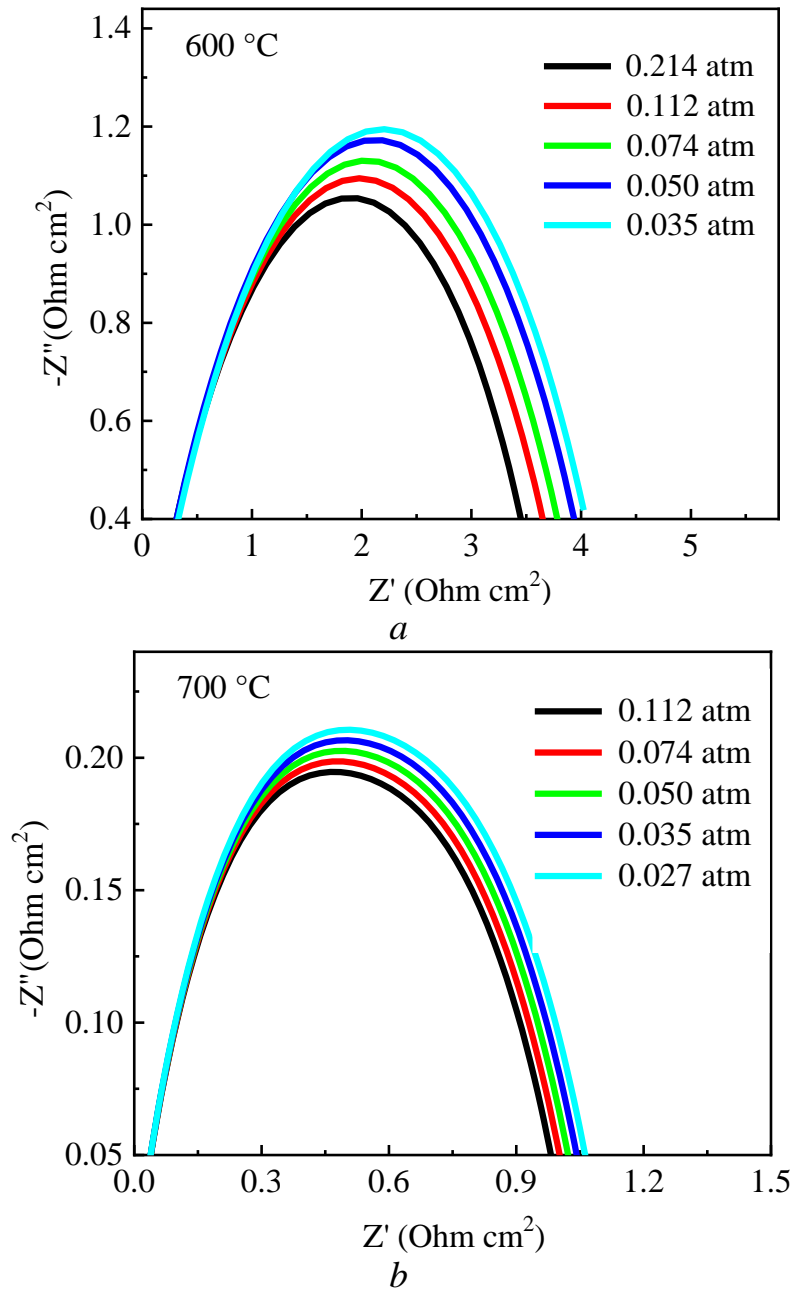
The 5+δ as a function of temperature in air for the SBSC cathode

Specimens	Calcination temperature (°C)	5+δ			
		200 °C	400 °C	600 °C	800 °C
SBSC91 [25]	1200	5.53	5.44	5.32	5.18
SBSC73 [25]	1200	5.62	5.55	5.36	5.22
SBSC55 [25]	1200	5.74	5.64	5.51	5.39
SBSC [this work]	1000	5.92	5.76	5.60	5.41

The calcination temperature has an impact on the oxygen content of the SBSC cathode. The oxygen content of the cathode with a calcination temperature of 1200 °C is smaller than that of a calcined at a temperature of 1000 °C. In the cathode with the calcination of 1200 °C, the oxygen content values were 5.74 (200 °C) and 5.39 (800 °C), while in the cathode with the calcination temperature 1000 °C the oxygen content values obtained were 5.92 and 5.41.

### 5. 3. OPP Half-Cell

Typical impedance spectra for symmetrical cells (SBSC|SDC|SBSC) were obtained by AC impedance spectroscopy. Fig. 5, shows the fitting data of impedance spectra for symmetrical cells measured at different temperatures such as *a* – 600 °C; *b* – 700 °C; and *c* – 800 °C, serially. While, the various OPPs was employed from 0.214–0.035 atm. The polarization resistance ( $R_p$ ) was a function of  $p(\text{O}_2)$  which is investigated under various temperatures between 600 °C to 800 °C with the OPPs ranged from 0.214 to 0.035 atm.





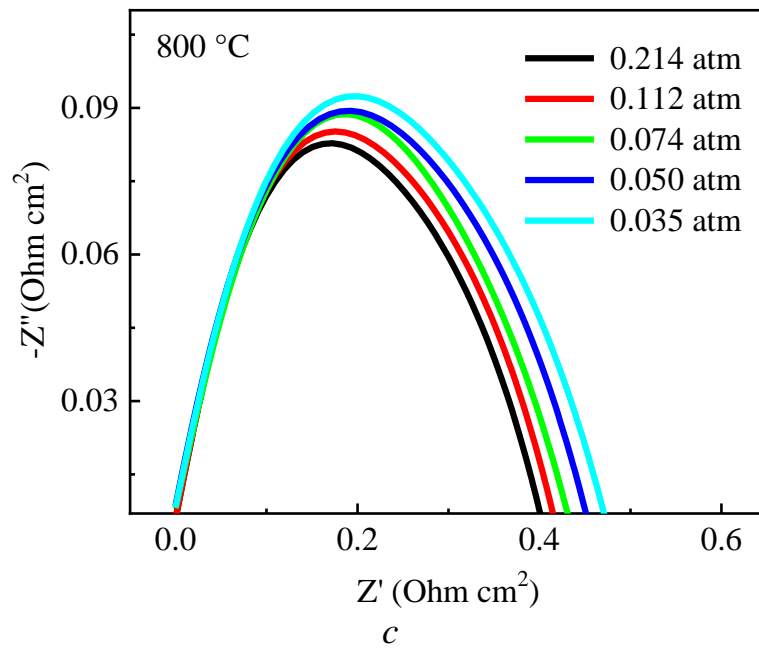


Fig. 5. The fitting data of impedance spectra for symmetrical cells measured at: *a* – 600 °C; *b* – 700 °C; *c* – 800 °C. The various OPPs from 0.214–0.035 atm

The  $R_p$  values increased with decreasing  $p(\text{O}_2)$  values due to the decrease in mobile interstitial oxygen at lower  $p(\text{O}_2)$  values. The fitting of the impedance spectrum for symmetrical cells using the Z-View program. The  $R_p$  value of the specimen was significantly reduced at 800 °C with an oxygen partial pressure (OPP) of 0.214 atm as presented in Fig. 6.

Table 4

Interfacial polarization resistance ( $R_p$ ) as a function of  $p(\text{O}_2)$  for SBSC|SDC|SBSC symmetrical cells

$p(\text{O}_2)$ (atm)	$R_p$ ( $\Omega\text{cm}^2$ )		
	600 °C	700 °C	800 °C
0.214	4.02	1.04	0.42
0.112	4.62	1.06	0.43
0.074	4.90	1.08	0.45
0.050	5.10	1.10	0.47
0.035	5.32	1.20	0.49

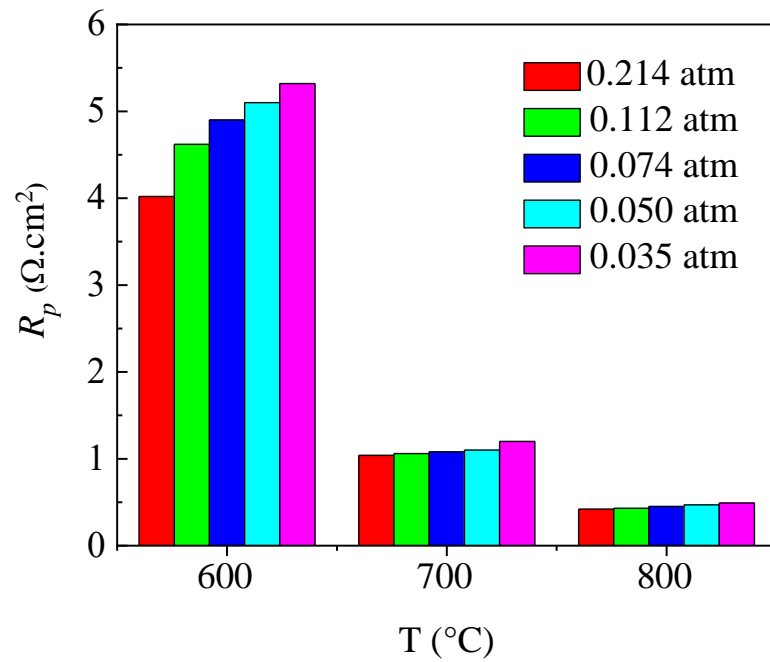


Fig. 6. The interfacial polarization resistance ( $R_p$ ) as a function of  $p(\text{O}_2)$  for SBSC|SDC|SBSC symmetrical cells at 600 °C, 700 °C, and 800 °C

The cathode cell performance is influenced by the values of the  $R_p$  obtained from the components. The high  $R_p$  values have a significant impact on SOFC performance. In general, the value of  $R_p$  has decreased with the increase in the working temperature of the SOFC. These conditions, the manufacture of SOFC components, especially the high density between layers (anode, electrolyte, and cathode), is of great concern to researchers.

#### 5. 4. Single-Cell Performance

Fig. 7 shows the single-cell performance of anode-supported Ni-SDC|SDC|SBSC was performed under air/humidified hydrogen (3 vol %  $\text{H}_2\text{O}$ ). Increasing temperature has an impact on increasing the current density and power density due to the thermally activated kinetic process [34]. Due to the same phenomenon, cell voltage increased at higher temperatures. Fig. 4 also indicates that the open-circuit voltages (OCVs) are 0.83, 0.81, and 0.84 at 425 °C, 450 °C, and 475 °C, respectively; these values are lower than the theoretical values.

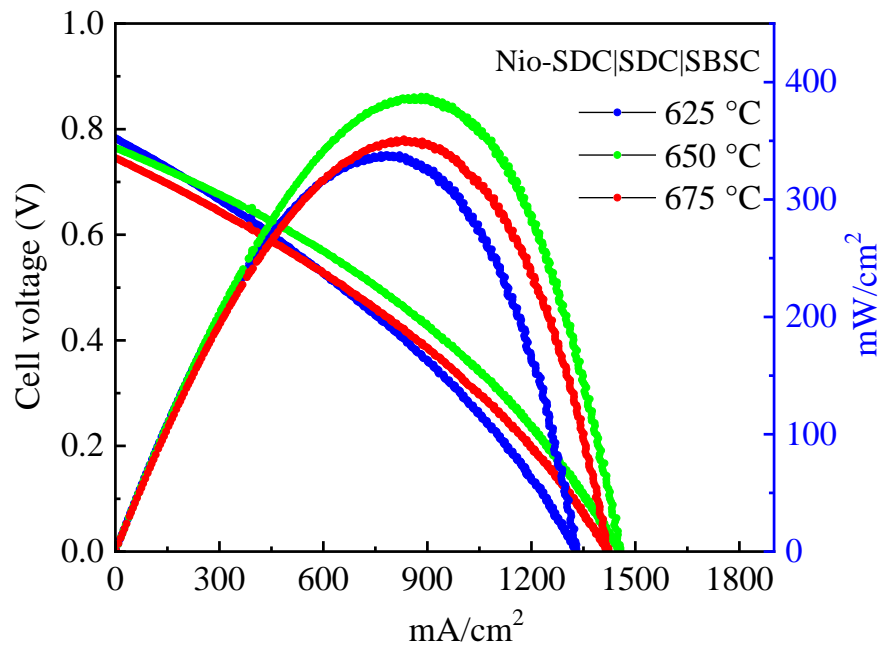
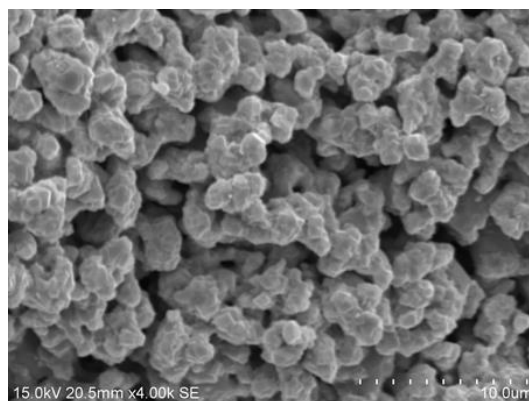


Fig. 7. The performance of a single cell of Ni-SDC|SDC|SBSC at temperatures ranging from 625 °C to 725 °C Fig. 7. The performance of a single cell of Ni-SDC|SDC|SBSC at temperatures ranging from 625 °C to 675 °C

The cathode performance in the SOFC cell as shown in Fig. 6, the power density at 650 °C exceeds that of the cell at 675 °C. This phenomenon needs to be analyzed more deeply because in general, the performance of SOFC cells increases with an increased operating temperature range between 600 °C and 800 °C. With these results, it can be stated that the SBSC oxide works well as a SOFC cathode at intermediate operating temperature.

### 5. 5. SEM Image

Fig. 8 displays the SEM images of *a* – cross-sectional image of the SBSC cathode in the SBSC|SDC|SBSC symmetrical-cell specimen and *b* – a top view of the SBSC cathode. In the symmetric cell, the cathode layer of SBSC was calcined in air for two h at 1000 °C. A uniform porous microstructure facilitates the gas diffusion of the cathode layer. A well-connected electrolyte–cathode interface determines low resistance in the solid oxide fuel cell.



*a*

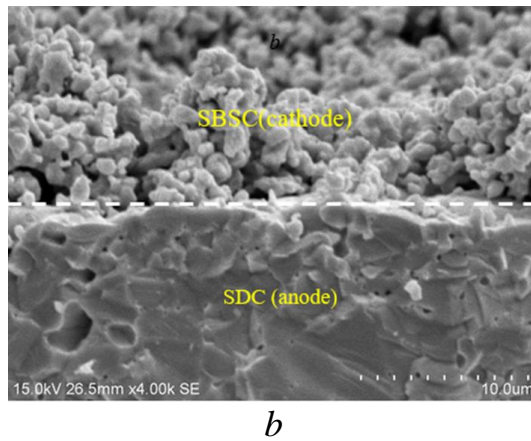


Fig. 8. SEM image: *a* – Cross-sectional SEM image of the SBSC cathode in the SBSC|SDC|SBSC symmetrical cell specimen prepared at 1000 °C for two h; *b* – a top view of the SBSC cathode

In Fig. 8, *b*, the adhesion between the SDC electrolyte and the SBSC cathode layer is quite good. The SBSC cathode grain size is distributed uniformly in the range of 1.5–2  $\mu\text{m}$  and is porous.

## 6. Discussion of experimental results

The XRD pattern of SBSC powder, which can be categorized into a tetragonal space group (P4/mmm) is as shown in Fig. 3, after calcining at 1000 °C for 6 h. There is a good compatibility level between the experimental data and calculated profiles, which shows that the cations are ordered well in the perovskite lattice arrangement between the  $\text{Sm}^{3+}$  and  $\text{Ba}^{2+}/\text{Sr}^{2+}$  ions [35].

The overall change in mass of the SBSC powder reached 8 % at temperatures of 125–800 °C. Previous data showed that the specimen was beginning to lose lattices oxygen significantly at a specific temperature [36]. A partial loss of oxygen lattices, along with a reduction in  $\text{Co}^{3+}$  to  $\text{Co}^{2+}$ , or  $\text{Co}^{4+}$  to  $\text{Co}^{3+}$ , and an increase in temperature, causes a decrease in weight loss during heating. Therefore, the oxygen content decreases with temperature [37, 38]. The high diffusivity regarding oxide ions and the increased surface activity of the ORRs might be due to a high oxygen content [39].

To clarify the polarization of the SBSC cathode resistance, the symmetrical cells test was carried out with various OPPs from 0.214–0.035 atm. From data, with increasing temperatures, the  $R_p$  values fell dramatically, suggesting that the SBSC sample ORR is a thermally activated process. The  $R_p$  values of the specimen reduced from  $4.02 \Omega\text{cm}^2$  at 600 °C to  $0.42 \Omega\text{cm}^2$  at 800 °C with an OPP of 0.214 atm as presented in Fig. 6. However, the  $R_p$  values increased significantly with a decreasing oxygen partial pressure. For instance, as the  $p(\text{O}_2)$  decreases from 0.214 to 0.035 atm, the  $R_p$  value increases from 4.02 to  $5.32 \Omega\text{cm}^2$  at a temperature of 600 °C. This study is consistent with results previously reported by Meng et al. regarding changes in polarization resistance to oxygen partial pressure [40]. The  $R_p$  values reflect cathodic behavior, including diffusion of oxygen at high temperatures in the gas phase, low-temperature ORR, and the surface of bulk diffusion/oxygen [41].

From single cell testing, ideally, the OCV of a cell should be similar to its 1.1 V theoretical value and should only small if affected by factors of operating conditions. Porosity impacts the leakage current when fuel/oxidants crossing the electrolyte membrane can cause low OCV values. The following equation can explain the concept of chemical defect:



Electrolyte-based materials with low electronic conductivity, such as SDC, may lead to a slight electron cross flow via the electrolyte. Alternatively,  $\text{Ce}^{4+}$  in SDC electrolytes is quickly reduced to  $\text{Ce}^{3+}$ , particularly at higher temperatures [29]. The power density values of the cell with an SBSC cathode are 336.1, 387.3, and 357.4  $\text{mW}/\text{cm}^2$  at 625 °C, 650 °C, and 675 °C, respectively. One method of improving cell performance is by modifying the cathode surface using electrolyte-based materials such as SDC. As previously reported, SDC nanoparticles implanted into the porous surface of the cathode produce a significant increase in the power density value [42].

Fig. 8 shows a cross-sectional view of SBSC|SDC from the prepared symmetrical cell and top surface SEM images. The SBSC cathode grain size is distributed uniformly in the range of 1.5–2  $\mu\text{m}$  and is porous. Better morphology is very helpful to ensure increased current, reduced  $R_p$  values, and rapid oxygen diffusion during SOFC operations. Also, the cathode structure's properties determine the cell's performance in processes such as kinetic reactions, mass transportation precesses, and charge transportation [43].

Overall, we have presented the SBSC perovskite oxide investigation in this report. However, a more comprehensive study is needed to improve SOFC performance, including thermal expansion testing to determine the degradation resistance between SOFC layers. In future work, we will focus on increasing the value of open-circuit voltage (OCV) using a bi-layer electrolyte of Ytria-stabilized Zirconia (YSZ)/Samaria doped Ceria (SDC) dense through pulsed laser deposition (PLD) technique. YSZ dense layer prepared by pulsed laser deposition (PLD) technique as a blocking layer improved the stability of the SDC electrolyte and inhibited electronic current leakage. This method is expected to increase the value of OCV and the single-cell performance.

## 7. Conclusions

1. The XRD structure of the SBSC cathode has been successfully categorized as double perovskite oxide by the solid-state reaction method. The double perovskite structure consists of the elements  $\text{Sm}^{3+}$ ,  $\text{Ba}^{2+}$  on the A-side and  $\text{Sr}^{2+}$ ,  $\text{Co}^{3+}$  on the B side.

2. The  $R_p$  values of the specimen decreased from 4.02  $\Omega\text{cm}^2$  at 600 °C to 0.42  $\Omega\text{cm}^2$  at 800 °C. The maximum power density of the single cell is 387.3  $\text{mW}/\text{cm}^2$  at 650 °C indicates that SBSC qualifies as the SOFC cathode material.

3. SBSC cathodes show good performance at intermediate operating

temperatures (600–800 °C).

### Acknowledgements

The authors are grateful for the financial support provided by Institut Teknologi Nasional Yogyakarta (Indonesia). The authors are also grateful for the financial support by A113 Laboratory of MSE (NDHU) and grand funded through MOST 106-2113-M-259-011 by the Ministry of Science and Technology of Taiwan.

### References

1. B.C.H. Steele, A. Heinzel. (2001). Materials for fuel-cell technologies. *Nature*, 414, 345–352. doi.org/10.1038/35104620.
2. N.Q. Minh. (1993). Ceramic fuel cell. *J Am Ceram Soc.*, 76, 563–588. doi.org/10.1111/j.1151-2916.1993.tb03645.x.
3. J.C. Ruiz-Molares, D. Marrero-Lo'pez, J. Canales-Va'zquez, J.T.S. Irvine. (2011). Symmetric and reversible solid oxide fuel cells. *RSC Adv.*, 1, 1403–1414. doi.org/10.1039/c1ra00284h.
4. S.J. Skinner. (2011). Recent advances in perovskite-type materials for solid oxide fuel cell cathodes. *Int. J. Inorg. Mater.*, 3, 113–121. doi.org/10.1016/s1466-6049(01)00004-6.
5. D.J.L. Brett, A. Atkinson, N.P. Brandon, S.J. Skinner. (2008). Intermediate temperature solid oxide fuel cells. *Chem Soc Rev.*, 37, 1568–1578. doi.org/10.1039/b612060c .
6. I. Susanto, D. M. Kamal, S. Ruswanto, R. Subarkah, F. Zainuri, S. Permana, J. W Soedarsono, A. Subardi, Y. P. Fu. (2020). Development of cobalt-free oxide ( $\text{Sm}_{0.5}\text{Sr}_{0.5}\text{Fe}_{0.8}\text{Cr}_{0.2}\text{O}_{3-\delta}$ ) of cathode for intermediate-temperature solid oxide fuel cells (IT-SOFCs). *Eastern-European Journal of Enterprise Technologies*, 6 (5 (108)), 15-20. https://doi.org/10.15587/1729-4061.2020.217282
7. H.Y. Liu, X.F. Zhu, M.J. Cheng, Y. Cong, W.S. Yang. (2011). Novel  $\text{Mn}_{1.5}\text{Co}_{1.5}\text{O}_4$  spinel cathodes for intermediate solid oxide fuel cells. *Chem Commun.*, 47, 2378–2380. doi.org/10.1039/c0cc04300a.
8. S.B. Adler. (2004). Factors governing oxygen reduction in solid oxide fuel cell cathodes. *Chem Rev.*, 104, 4791–4844. doi.org/10.1021/cr020724o.
9. Y. Takeda, R. Kanno, M. Noda, Y. Tomida, O. Yamamoto. (1987). Cathodic polarization phenomena of perovskite oxide electrodes with stabilized zirconia. *Journal of The Electrochemical Society volume*, 134, 2656–2661. doi.org/10.1149/1.2100267.
10. S.B. Adler, J.A. Lane, B.C.H. Steele. (1996). Electrode kinetics of porous mixed-conducting oxygen electrodes. *J Electrochem Soc.*, 143, 3554–3564. doi.org/10.1149/1.1837252.
11. A. Subardi, M.H. Cheng, Y.P. Fu. (2014). Chemical bulk diffusion and electrochemical properties of  $\text{SmBa}_{0.6}\text{Sr}_{0.4}\text{Co}_2\text{O}_{5+\delta}$  cathode for intermediate solid oxide fuel cells. *Int J Hydrogen Energy*, 39, 20783–20790. doi.org/10.1016/j.ijhydene.2014.06.134.
12. F. Zhao, S. Wang, K. Brinkman, F. Chen. (2010). Layered perovskite  $\text{PrBa}_{0.5}\text{Sr}_{0.5}\text{Co}_2\text{O}_{5+\delta}$  as high performance cathode for solid oxide fuel cells using oxide

proton-conducting electrolyte. *J Power Sources*, 195, 5468–5473. doi.org/10.1016/j.jpowsour.2010.03.088.

13. Q. Zhou, T. He, Y. Ji. (2008). SmBaCo<sub>2</sub>O<sub>5+δ</sub> double-perovskite structure cathode material for intermediate-temperature solid-oxide fuel cells. *J Power Sources*, 185, 754–758. doi.org/10.1016/j.jpowsour.2008.07.064.

14. A. Tarancon, M. Burriel, J. Santiso, S.J., Skinner, J.A. Kilner. (2010). Advances in layered oxide cathodes for intermediate temperature solid oxide fuel cells. *J Mater Chem.*, 20, 3799–3813. doi.org/10.1039/b922430k.

15. D.J. Chen, R. Ran, K. Zhang, J. Wang, Z.P. Shao. (2009). Intermediate-temperature electrochemical performance of a polycrystalline PrBaCo<sub>2</sub>O<sub>5+δ</sub> cathode on samarium-doped ceria electrolyte. *J Power Sources*, 188, 96–105. doi.org/10.1016/j.jpowsour.2008.11.045.

16. C. Kuroda, K. Zheng, K. Swierczek. (2013). Characterization of novel GdBa<sub>0.5</sub>Sr<sub>0.5</sub>Co<sub>2-x</sub>Fe<sub>x</sub>O<sub>5+δ</sub> perovskites for application in IT-SOFC cells. *Int. J. Hydrogen Energy*, 38, 1027–1038. doi.org/10.1016/j.ijhydene.2012.10.085.

17. A. Tarancon, A. Morata, G. Dezanneau, S.J. Skinner, J.A. Kilner, A. Estrade, F.H. Ramirez, F. Peiro, J.R. Morante. (2007). GdBaCo<sub>2</sub>O<sub>5+δ</sub> layered perovskite as an intermediate temperature solid oxide fuel cell cathode. *J. Power Sources*, 174, 255–263. doi.org/10.1016/j.jpowsour.2007.08.077

18. A. Chang, S.J. Skinner, J.A. Kilner. (2006). Electrical properties of GdBaCo<sub>2</sub>O<sub>5+δ</sub> for SOFC applications. *Solid State Ionics*, 177, 2009–2011. doi.org/10.1016/j.ssi.2006.05.047.

19. H. Gu, H. Chen, L. Gao, Y. Zheng, X. Zhu, L. Guo. (2009). Oxygen reduction mechanism of NdBaCo<sub>2</sub>O<sub>5+δ</sub> cathode for intermediate-temperature solid oxide fuel cells under cathodic polarization. *Int. J. Hydrogen Energy*, 34, 2416–2420. doi.org/10.1016/j.ijhydene.2009.01.003.

20. X. Kong, X. Ding. (2011). Novel layered perovskite SmBaCu<sub>2</sub>O<sub>5+δ</sub> as a potential cathode for intermediate temperature solid oxide fuel cells. *Int. J. Hydrogen Energy*, 36, 15715–15721. doi.org/10.1016/j.ijhydene.2011.09.035.

21. J.H. Kim, Y. Kim, P.A. Connor, J.T.S. Irvine, J. Bae, W. Zhou. (2009). Structural thermal and electrochemical properties of layered perovskite SmBaCo<sub>2</sub>O<sub>5+δ</sub>, a potential cathode material for intermediate-temperature solid oxide fuel cells. *J. Power Sources*, 194, 704–711. doi.org/10.1016/j.jpowsour.2009.06.024.

22. W. Liu, C. Yang, X. Wu, H. Gao, Z. Chen. (2011). Oxygen relaxation and phase transition in GdBaCo<sub>2</sub>O<sub>5+δ</sub> oxide. *Solid State Ionics*, 192, 245–247. doi.org/10.1016/j.ssi.2010.04.028.

23. J.H. Kim, L. Moggi, F. Prado, A. Caneiro, J.A. Alonso, A. Manthiram. (2009). High temperature crystal chemistry and oxygen permeation properties of the mixed ionic-electronic conductors LnBaCo<sub>2</sub>O<sub>5+δ</sub> (Ln=Lanthanide). *J. Electrochem. Soc.*, 156, B1376–1382. doi.org/10.1149/1.3231501.

24. A. Subardi, C. Ching-Cheng, C. Meng-Hsien, C. Wen-Ku, Y.P. Fu. (2016). Electrical, thermal and electrochemical properties of SmBa<sub>1-x</sub>Sr<sub>x</sub>Co<sub>2</sub>O<sub>5+δ</sub> cathode materials for intermediate-temperature solid oxide fuel cells. *Electrochim Acta*, 204, 118–27. doi.org/10.1016/j.electacta.2016.04.069.

25. S. Lu, G. Long, X. Meng, Y. Ji, B. Lu, H. Zhao. (2012).

PrBa<sub>0.5</sub>Sr<sub>0.5</sub>Co<sub>2</sub>O<sub>5+δ</sub> as cathode material based on LSGM and GDC electrolyte for intermediate-temperature solid oxide fuel cells. *Int. J. Hydrogen Energy*, 37, 5914–5919. doi.org/10.1016/j.ijhydene.2011.12.134.

26. Y.P. Fu, S.B. Wen, C.H. Lu. (2008). Preparation and characterization of Samaria-doped ceria electrolyte materials for solid oxide fuel cells. *J Am Ceram Soc.*, 91, 127–31. doi.org/10.1111/j.1551-2916.2007.01923.x.

27. M. Kuhn, J.J. Kim, S.R. Bishop, H.L. Tuller. (2013). Oxygen nonstoichiometry and defect chemistry of perovskite-structured Ba<sub>x</sub>Sr<sub>1-x</sub>Ti<sub>1-y</sub>Fe<sub>y</sub>O<sub>3-y/2+δ</sub>. *Chem Mater.*, 25, 2970–75. doi.org/10.1021/cm400546z.

28. Y.P. Fu, J. Ouyang, C.H. Li, S.H. Hu. (2013). Chemical bulk diffusion coefficient of Sm<sub>0.5</sub>Sr<sub>0.5</sub>CoO<sub>3-δ</sub> cathode for solid oxide fuel cells. *J Power Sources*, 240, 168–77. doi.org/10.1016/j.jpowsour.2013.03.138.

29. T.V. Aksenova, L.Y. Gavrilova, A.A. Yaremchenko, V.A. Cherepanov, V.V. Kharton. (20120). Oxygen nonstoichiometry, thermal expansion, and high-temperature electrical properties of layered NdBaCo<sub>2</sub>O<sub>5+δ</sub> and SmBaCo<sub>2</sub>O<sub>5+δ</sub>. *Mater Res Bull*, 45, 1288–1292. doi.org/10.1016/j.materresbull.2010.05.004.

30. K. Zhang, L. Ge, R. Ran, Z. Shao, S. Liu. (2008). Synthesis, characterization, and evaluation of cation-ordered LnBaCo<sub>2</sub>O<sub>5+δ</sub> as materials of oxygen permeation membranes and cathodes of SOFCs. *Acta Mater.*, 56, 4876–4889. doi.org/10.1016/j.actamat.2008.06.004.

31. K. Jiyoun, C. Sihyuk, P. Seonhye, K. Changmin, S. Jeeyoung, K. Guntae. (2013). Effect of Mn on the electrochemical properties of a layered perovskite NdBa<sub>0.5</sub>Sr<sub>0.5</sub>Co<sub>2-x</sub>Mn<sub>x</sub>O<sub>5+δ</sub> (x=0, 0.25, and 0.5) for intermediate-temperature solid oxide fuel cells. *Electrochim Acta*, 112, 712–718. doi.org/10.1016/j.electacta.2013.09.014.

32. A. Subardi, YP. Fu. (2017). Electrochemical and thermal properties of SmBa<sub>0.5</sub>Sr<sub>0.5</sub>Co<sub>2</sub>O<sub>5+δ</sub> cathode impregnated with Ce<sub>0.8</sub>Sm<sub>0.2</sub>O<sub>1.90</sub> nanoparticles for intermediate temperature solid oxide fuel cells. *Int J Hydrogen Energy*, 42, 24338–24346. doi.org/10.1016/j.ijhydene.2017.08.010.

33. M. West, A. Manthiram. (2013). Layered LnBa<sub>1-x</sub>Sr<sub>x</sub>CoCuO<sub>5+δ</sub> (Ln=Nd and Gd) perovskite cathodes for intermediate temperature solid oxide fuel cell *Int. J Hydrogen Energy*, 38, 3364–72. doi.org/10.1016/j.ijhydene.2012.12.133.

34. M.B. Choi, K.T. Lee, H.S. Yoon, S.Y. Jeon, E.D. Wachsman, S.J. Song. (2012). Electrochemical properties of ceria-based intermediate temperature solid oxide fuel cells using microwave heated La<sub>0.1</sub>Sr<sub>0.9</sub>Co<sub>0.8</sub>Fe<sub>0.2</sub>O<sub>3-δ</sub> as a cathode. *J Power Sources*, 220, 377–382. doi.org/10.1016/j.jpowsour.2012.07.122.

35. A. Jun, J. Shin, G. Kim. (2013). High redox and performance stability of layered SmBa<sub>1-x</sub>Sr<sub>x</sub>Co<sub>1.5</sub>Cu<sub>0.25</sub>O<sub>5+δ</sub> perovskite cathodes for intermediate-temperature solid oxide fuel cells. *Phys Chem Phys.*, 15, 19906–19912. doi.org/10.1039/c3cp53883d.

36. G.C. Kostoglou, N. Vasilakos, C. Ftikos. (1998). Crystal structure, thermal and electrical properties of Pr<sub>1-x</sub>Sr<sub>x</sub>CoO<sub>3-δ</sub> (x=0, 0.15, 0.3, 0.4, 0.5) perovskite oxides. *Solid State Ionics*, 106, 207–218. doi.org/10.1016/s0167-2738(97)00506-7.

37. P. Meuffels. (2007). Propane gas sensing with high density SrTi<sub>0.6</sub>Fe<sub>0.4</sub>O<sub>3-δ</sub> ceramics evaluated by thermogravimetric analysis. *J Eur Ceram Soc.*, 27, 285–290.



doi.org/10.1016/j.jeurceramsoc.2006.05.078.

38. S. Lia, W. Jin, N. Xu, J. Shi. (2001). Mechanical strength, and oxygen and electronic transport properties of  $\text{SrCo}_{0.4}\text{Fe}_{0.6}\text{O}_{3-\delta}$  -YSZ membranes. *J Membr Sci.*, 186, 195–204. doi.org/10.1016/s0376-7388(00)00681-5.

39. G. Kim, S. Wang, A.J. Jacobson, L. Reimus, P. Brodersen, C.A. Mims. (2007). Rapid oxygen ion diffusion and surface exchange kinetics in  $\text{PrBaCo}_2\text{O}_{5+\delta}$  with a perovskite-related structure and ordered A cations. *J Mater Chem.*, 17, 2500–2505. doi.org/10.1039/b618345j.

40. M. Fuchang, X. Tian, W. Jingping, S. Zhan, Z. Hui, B. Jean-Marc. (2014). Evaluation of layered perovskites  $\text{YBa}_{1-x}\text{Sr}_x\text{Co}_2\text{O}_{5+\delta}$  as cathodes for intermediate-temperature solid oxide fuel cells. *Int J Hydrogen Energy*, 39, 4531–4543. doi.org/10.1016/j.ijhydene.2014.01.008.

41. S.W. Baek, J.H. Kim, J. Bae. (2008). Characteristics of  $\text{ABO}_3$  and  $\text{A}_2\text{BO}_4$  (A=Sm, Sr; B=Co, Fe, Ni) samarium oxide system as cathode materials for intermediate temperature-operating solid oxide fuel cell. *Solid State Ionics*, 179, 1570–1574. doi.org/10.1016/j.ssi.2007.12.010.

42. J. H. Nam, D.H. Jeon. (2006). A Comprehensive microscale model for transport and reaction in intermediate temperature solid oxide fuel cell. *Electrochim Acta*, 51, 3446–3460. doi.org/10.1016/j.electacta.2005.09.041.

43. M. Anderson, J. Yuan, B. Sunden. Review on modeling development for multiscale chemical reactions coupled transport phenomena in the solid oxide fuel cell. *Appl Energy*, 87, 1461–1476. doi.org/10.1016/j.apenergy.2009.11.013.

## References

1. B.C.H. Steele, A. Heinzl. (2001). Materials for fuel-cell technologies. *Nature*, 414, 345–352. doi.org/10.1038/35104620.

2. N.Q. Minh. (1993). Ceramic fuel cell. *J Am Ceram Soc.*, 76, 563–588. doi.org/10.1111/j.1151-2916.1993.tb03645.x.

3. J.C. Ruiz-Molares, D. Marrero-López, J. Canales-Vázquez, J.T.S. Irvine. (2011). Symmetric and reversible solid oxide fuel cells. *RSC Adv.*, 1, 1403–1414. doi.org/10.1039/c1ra00284h.

4. S.J. Skinner. (2011). Recent advances in perovskite-type materials for solid oxide fuel cell cathodes. *Int. J. Inorg. Mater.*, 3, 113–121. doi.org/10.1016/s1466-6049(01)00004-6.

5. D.J.L. Brett, A. Atkinson, N.P. Brandon, S.J. Skinner. (2008). Intermediate temperature solid oxide fuel cells. *Chem Soc Rev.*, 37, 1568–1578. doi.org/10.1039/b612060c .

6. I. Susanto, D. M. Kamal, S. Ruswanto, R. Subarkah, F. Zainuri, S. Permana, J. W Soedarsono, A. Subardi, Y. P. Fu. (2020). Development of cobalt-free oxide ( $\text{Sm}_{0.5}\text{Sr}_{0.5}\text{Fe}_{0.8}\text{Cr}_{0.2}\text{O}_{3-\delta}$ ) of cathode for intermediate-temperature solid oxide fuel cells (IT-SOFCs). *Eastern-European Journal of Enterprise Technologies*, 6 (5 (108)), 15-20. <https://doi.org/10.15587/1729-4061.2020.217282>

7. H.Y. Liu, X.F. Zhu, M.J. Cheng, Y. Cong, W.S. Yang. (2011). Novel  $\text{Mn}_{1.5}\text{Co}_{1.5}\text{O}_4$  spinel cathodes for intermediate solid oxide fuel cells. *Chem Commun.*, 47, 2378–2380. doi.org/10.1039/c0cc04300a.

8. S.B. Adler. (2004). Factors governing oxygen reduction in solid oxide fuel cell cathodes. *Chem Rev.*, 104, 4791–4844. doi.org/10.1021/cr020724o.
9. Y. Takeda, R. Kanno, M. Noda, Y. Tomida, O. Yamamoto. (1987). Cathodic polarization phenomena of perovskite oxide electrodes with stabilized zirconia. *Journal of The Electrochemical Society* volume, 134, 2656–2661. doi.org/10.1149/1.2100267.
10. S.B. Adler, J.A. Lane, B.C.H. Steele. (1996). Electrode kinetics of porous mixed-conducting oxygen electrodes. *J Electrochem Soc.*, 143, 3554–3564. doi.org/10.1149/1.1837252.
11. A. Subardi, M.H. Cheng, Y.P. Fu. (2014). Chemical bulk diffusion and electrochemical properties of  $\text{SmBa}_{0.6}\text{Sr}_{0.4}\text{Co}_2\text{O}_{5+\delta}$  cathode for intermediate solid oxide fuel cells. *Int J Hydrogen Energy*, 39, 20783–20790. doi.org/10.1016/j.ijhydene.2014.06.134.
12. F. Zhao, S. Wang, K. Brinkman, F. Chen. (2010). Layered perovskite  $\text{PrBa}_{0.5}\text{Sr}_{0.5}\text{Co}_2\text{O}_{5+\delta}$  as high performance cathode for solid oxide fuel cells using oxide proton-conducting electrolyte. *J Power Sources*, 195, 5468–5473. doi.org/10.1016/j.jpowsour.2010.03.088.
13. Q. Zhou, T. He, Y. Ji. (2008).  $\text{SmBaCo}_2\text{O}_{5+\delta}$  double-perovskite structure cathode material for intermediate-temperature solid-oxide fuel cells. *J Power Sources*, 185, 754–758. doi.org/10.1016/j.jpowsour.2008.07.064.
14. A. Tarancon, M. Burriel, J. Santiso, S.J., Skinner, J.A. Kilner. (2010). Advances in layered oxide cathodes for intermediate temperature solid oxide fuel cells. *J Mater Chem.*, 20, 3799–3813. doi.org/10.1039/b922430k.
15. D.J. Chen, R. Ran, K. Zhang, J. Wang, Z.P. Shao. (2009). Intermediate-temperature electrochemical performance of a polycrystalline  $\text{PrBaCo}_2\text{O}_{5+\delta}$  cathode on samarium-doped ceria electrolyte. *J Power Sources*, 188, 96–105. doi.org/10.1016/j.jpowsour.2008.11.045.
16. C. Kuroda, K. Zheng, K. Swierczek. (2013). Characterization of novel  $\text{GdBa}_{0.5}\text{Sr}_{0.5}\text{Co}_{2-x}\text{FexO}_{5+\delta}$  perovskites for application in IT-SOFC cells. *Int. J. Hydrogen Energy*, 38, 1027–1038. doi.org/10.1016/j.ijhydene.2012.10.085.
17. A. Tarancon, A. Morata, G. Dezanneau, S.J. Skinner, J.A. Kilner, A. Estrade', F.H. Ramirez, F. Peiro, J.R. Morante. (2007).  $\text{GdBaCo}_2\text{O}_{5+\delta}$  layered perovskite as an intermediate temperature solid oxide fuel cell cathode. *J. Power Sources*, 174, 255–263. doi.org/10.1016/j.jpowsour.2007.08.077
18. A. Chang, S.J. Skinner, J.A. Kilner. (2006). Electrical properties of  $\text{GdBaCo}_2\text{O}_{5+\delta}$  for SOFC applications. *Solid State Ionics*, 177, 2009–2011. doi.org/10.1016/j.ssi.2006.05.047.
19. H. Gu, H. Chen, L. Gao, Y. Zheng, X. Zhu, L. Guo. (2009). Oxygen reduction mechanism of  $\text{NdBaCo}_2\text{O}_{5+\delta}$  cathode for intermediate-temperature solid oxide fuel cells under cathodic polarization. *Int. J. Hydrogen Energy*, 34, 2416–2420. doi.org/10.1016/j.ijhydene.2009.01.003.
20. X. Kong, X. Ding. (2011). Novel layered perovskite  $\text{SmBaCu}_2\text{O}_{5+\delta}$  as a potential cathode for intermediate temperature solid oxide fuel cells. *Int. J. Hydrogen Energy*, 36, 15715–15721. doi.org/10.1016/j.ijhydene.2011.09.035.
21. J.H. Kim, Y. Kim, P.A. Connor, J.T.S. Irvine, J. Bae, W. Zhou. (2009).

Structural thermal and electrochemical properties of layered perovskite  $\text{SmBaCo}_2\text{O}_{5+\delta}$ , a potential cathode material for intermediate-temperature solid oxide fuel cells. *J. Power Sources*, 194, 704–711. doi.org/10.1016/j.jpowsour.2009.06.024.

22. W. Liu, C. Yang, X. Wu, H. Gao, Z. Chen. (2011). Oxygen relaxation and phase transition in  $\text{GdBaCo}_2\text{O}_{5+\delta}$  oxide. *Solid State Ionics*, 192, 245–247. doi.org/10.1016/j.ssi.2010.04.028.

23. J.H. Kim, L. Mogni, F. Prado, A. Caneiro, J.A. Alonso, A. Manthiram. (2009). High temperature crystal chemistry and oxygen permeation properties of the mixed ionic-electronic conductors  $\text{LnBaCo}_2\text{O}_{5+\delta}$  (Ln=Lanthanide). *J. Electrochem. Soc.*, 156, B1376–1382. doi.org/10.1149/1.3231501.

24. A. Subardi, C. Ching-Cheng, C. Meng-Hsien, C. Wen-Ku, Y.P. Fu. (2016). Electrical, thermal and electrochemical properties of  $\text{SmBa}_{1-x}\text{Sr}_x\text{Co}_2\text{O}_{5+\delta}$  cathode materials for intermediate-temperature solid oxide fuel cells. *Electrochim Acta*, 204, 118–27. 10.1016/j.electacta.2016.04.069.

25. S. Lu, G. Long, X. Meng, Y. Ji, B. Lu, H. Zhao. (2012).  $\text{PrBa}_{0.5}\text{Sr}_{0.5}\text{Co}_2\text{O}_{5+\delta}$  as cathode material based on LSGM and GDC electrolyte for intermediate-temperature solid oxide fuel cells. *Int. J. Hydrogen Energy*, 37, 5914–5919. doi.org/10.1016/j.ijhydene.2011.12.134.

26. Y.P. Fu, S.B. Wen, C.H. Lu. (2008). Preparation and characterization of Samaria-doped ceria electrolyte materials for solid oxide fuel cells. *J Am Ceram Soc.*, 91, 127–31. doi.org/10.1111/j.1551-2916.2007.01923.x.

27. M. Kuhn, J.J. Kim, S.R. Bishop, H.L. Tuller. (2013). Oxygen nonstoichiometry and defect chemistry of perovskite-structured  $\text{Ba}_x\text{Sr}_{1-x}\text{Ti}_{1-y}\text{Fe}_y\text{O}_{3-y/2+\delta}$ . *Chem Mater.*, 25, 2970–75. doi.org/10.1021/cm400546z.

28. Y.P. Fu, J. Ouyang, C.H. Li, S.H. Hu. (2013). Chemical bulk diffusion coefficient of  $\text{Sm}_{0.5}\text{Sr}_{0.5}\text{CoO}_{3-\delta}$  cathode for solid oxide fuel cells. *J Power Sources*, 240, 168–77. doi.org/10.1016/j.jpowsour.2013.03.138.

29. T.V. Aksenova, L.Y. Gavrilova, A.A. Yaremchenko, V.A. Cherepanov, V.V. Kharton. (20120). Oxygen nonstoichiometry, thermal expansion, and high-temperature electrical properties of layered  $\text{NdBaCo}_2\text{O}_{5+\delta}$  and  $\text{SmBaCo}_2\text{O}_{5+\delta}$ . *Mater Res Bull*, 45, 1288–1292. doi.org/10.1016/j.materresbull.2010.05.004.

30. K. Zhang, L. Ge, R. Ran, Z. Shao, S. Liu. (2008). Synthesis, characterization, and evaluation of cation-ordered  $\text{LnBaCo}_2\text{O}_{5+\delta}$  as materials of oxygen permeation membranes and cathodes of SOFCs. *Acta Mater.*, 56, 4876–4889. doi.org/10.1016/j.actamat.2008.06.004.

31. K. Jiyoun, C. Sihyuk, P. Seonhye, K. Changmin, S. Jeeyoung, K. Guntae. (2013). Effect of Mn on the electrochemical properties of a layered perovskite  $\text{NdBa}_{0.5}\text{Sr}_{0.5}\text{Co}_{2-x}\text{Mn}_x\text{O}_{5+\delta}$  ( $x=0, 0.25, \text{ and } 0.5$ ) for intermediate-temperature solid oxide fuel cells. *Electrochim Acta*, 112, 712–718. doi.org/10.1016/j.electacta.2013.09.014.

32. A. Subardi, Y.P. Fu. (2017). Electrochemical and thermal properties of  $\text{SmBa}_{0.5}\text{Sr}_{0.5}\text{Co}_2\text{O}_{5+\delta}$  cathode impregnated with  $\text{Ce}_{0.8}\text{Sm}_{0.2}\text{O}_{1.90}$  nanoparticles for intermediate temperature solid oxide fuel cells. *Int J Hydrogen Energy*, 42, 24338–24346. doi.org/10.1016/j.ijhydene.2017.08.010.

33. M. West, A. Manthiram. (2013). Layered  $\text{LnBa}_{1-x}\text{Sr}_x\text{CoCuO}_{5+\delta}$  (Ln=Nd

and Gd) perovskite cathodes for intermediate temperature solid oxide fuel cell Int. J Hydrogen Energy, 38, 3364–72. doi.org/10.1016/j.ijhydene.2012.12.133.

34. M.B. Choi, K.T. Lee, H.S. Yoon, S.Y. Jeon, E.D. Wachsman, S.J. Song. (2012). Electrochemical properties of ceria-based intermediate temperature solid oxide fuel cells using microwave heated  $\text{La}_{0.1}\text{Sr}_{0.9}\text{Co}_{0.8}\text{Fe}_{0.2}\text{O}_{3-\delta}$  as a cathode. J Power Sources, 220, 377–382. doi.org/10.1016/j.jpowsour.2012.07.122.

35. A. Jun, J. Shin, G. Kim. (2013). High redox and performance stability of layered  $\text{SmBa}_{1-x}\text{Sr}_x\text{Co}_{1.5}\text{Cu}_{0.25}\text{O}_{5+\delta}$  perovskite cathodes for intermediate-temperature solid oxide fuel cells. Phys Chem Phys., 15, 19906–19912. doi.org/10.1039/c3cp53883d.

36. G.C. Kostoglou, N. Vasilakos, C. Ftikos. (1998). Crystal structure, thermal and electrical properties of  $\text{Pr}_{1-x}\text{Sr}_x\text{CoO}_{3-\delta}$  ( $x=0, 0.15, 0.3, 0.4, 0.5$ ) perovskite oxides. Solid State Ionics, 106, 207–218. doi.org/10.1016/s0167-2738(97)00506-7.

37. P. Meuffels. (2007). Propane gas sensing with high density  $\text{SrTi}_{0.6}\text{Fe}_{0.4}\text{O}_{3-\delta}$  ceramics evaluated by thermogravimetric analysis. J Eur Ceram Soc., 27, 285–290. doi.org/10.1016/j.jeurceramsoc.2006.05.078.

38. S. Lia, W. Jin, N. Xu, J. Shi. (2001). Mechanical strength, and oxygen and electronic transport properties of  $\text{SrCo}_{0.4}\text{Fe}_{0.6}\text{O}_{3-\delta}$ -YSZ membranes. J Membr Sci., 186, 195–204. doi.org/10.1016/s0376-7388(00)00681-5.

39. G. Kim, S. Wang, A.J. Jacobson, L. Reimus, P. Brodersen, C.A. Mims. (2007). Rapid oxygen ion diffusion and surface exchange kinetics in  $\text{PrBaCo}_2\text{O}_{5+\delta}$  with a perovskite-related structure and ordered A cations. J Mater Chem., 17, 2500–2505. doi.org/10.1039/b618345j.

40. M. Fuchang, X. Tian, W. Jingping, S. Zhan, Z. Hui, B. Jean-Marc. (2014). Evaluation of layered perovskites  $\text{YBa}_{1-x}\text{Sr}_x\text{Co}_2\text{O}_{5+\delta}$  as cathodes for intermediate-temperature solid oxide fuel cells. Int J Hydrogen Energy, 39, 4531–4543. doi.org/10.1016/j.ijhydene.2014.01.008.

41. S.W. Baek, J.H. Kim, J. Bae. (2008). Characteristics of  $\text{ABO}_3$  and  $\text{A}_2\text{BO}_4$  ( $A=\text{Sm, Sr}$ ;  $B=\text{Co, Fe, Ni}$ ) samarium oxide system as cathode materials for intermediate temperature-operating solid oxide fuel cell. Solid State Ionics, 179, 1570–1574. doi.org/10.1016/j.ssi.2007.12.010.

42. J. H. Nam, D.H. Jeon. (2006). A Comprehensive microscale model for transport and reaction in intermediate temperature solid oxide fuel cell. Electrochim Acta, 51, 3446–3460. doi.org/10.1016/j.electacta.2005.09.041.

43. M. Anderson, J. Yuan, B. Sunden. Review on modeling development for multiscale chemical reactions coupled transport phenomena in the solid oxide fuel cell. Appl Energy, 87, 1461–1476. doi.org/10.1016/j.apenergy.2009.11.013.

Adi Subardi

Doctor of Materials Science and Engineering, Assistance Professor

Department of Mechanical Engineering

Institut Teknologi Nasional Yogyakarta

Jl Babarsari Caturtunggal, Depok, Sleman, Daerah Istimewa Yogyakarta, Indonesia, 55281

E-mail: subardi@itny.ac.id

Contact phone: +6282133167082

The number of articles in international databases: 9

H-index: 4

ORCID: <https://orcid.org/0000-0003-0867-3624>

[https://www.researchgate.net/profile/Adi\\_Subardi](https://www.researchgate.net/profile/Adi_Subardi)

[https://scholar.google.com/scholar?hl=id&as\\_sdt=0 %2C5&q=adi+subardi&btnG](https://scholar.google.com/scholar?hl=id&as_sdt=0%2C5&q=adi+subardi&btnG)

Iwan Susanto

Doctor of Materials Science and Engineering, Assistance Professor

Department of Mechanical Engineering

Politeknik Negeri Jakarta

Jl. Prof. DR. G.A. Siwabessy, Kukusan, Kecamatan Beji, Kota Depok, Jawa Barat, Indonesia, 16424

E-mail: iwan.susanto@mesin.pnj.ac.id

Contact phone: +6281932421764, +62217863530

The number of articles in international databases: 6

H-index: 3

ORCID: <http://orcid.org/0000-0001-7120-0374>

[https://www.researchgate.net/profile/Iwan\\_Susanto3](https://www.researchgate.net/profile/Iwan_Susanto3)

Ratna Kartikasari

Doctor of Mechanical Engineering, Associate Professor

Department of Mechanical Engineering

Institut Teknologi Nasional Yogyakarta

Jl Babarsari Caturtunggal, Depok, Sleman, Daerah Istimewa Yogyakarta, Indonesia, 55281

E-mail: ratna@itny.ac.id

Contact phone: +6281392019208

The number of articles in international databases: 4

H-index: 2

ORCID: <https://orcid.org/0000-0001-8859-3258>

[https://www.researchgate.net/profile/Ratna\\_Kartikasari](https://www.researchgate.net/profile/Ratna_Kartikasari)

[https://scholar.google.com/scholar?hl=id&as\\_sdt=0 %2C5&q=ratna+kartikasari&oq=Ratna+Kartika](https://scholar.google.com/scholar?hl=id&as_sdt=0%2C5&q=ratna+kartikasari&oq=Ratna+Kartika)

Tugino Tugino

Master of Electrical Engineering, Associate Professor

Department of Electrical Engineering

Institut Teknologi Nasional Yogyakarta

Jl Babarsari Caturtunggal, Depok, Sleman, Daerah Istimewa Yogyakarta, Indonesia, 55281

E-mail: tugino@itny.ac.id

Contact phone: +62 81578873090

The number of articles in international databases: -

H-index: -

ORCID: <https://orcid.org/0000-0003-0297-088X>

Hasta Kuntara

Master of Mechanical Engineering, Assistance Professor

Department of Mechanical Engineering

Institut Teknologi Nasional Yogyakarta

Jl Babarsari Caturtunggal, Depok, Sleman, Daerah Istimewa Yogyakarta, Indonesia, 55281

E-mail: [hasta@itny.ac.id](mailto:hasta@itny.ac.id)

Contact phone: + 6285728856654

The number of articles in international databases: -

H-index: -

ORCID: <https://orcid.org/0000-0002-3518-0692>

Andy Erwin Wijaya

Doctor of Mining Engineering, Assistance Professor

Department of Mining Engineering,

Institut Teknologi Nasional Yogyakarta

Jl Babarsari Caturtunggal, Depok, Sleman, Daerah Istimewa Yogyakarta, Indonesia, 55281

E-mail: [andyerwin@itny.ac.id](mailto:andyerwin@itny.ac.id)

Contact phone: +6282300182053

The number of articles in international databases: -

H-index: -

ORCID: <https://orcid.org/0000-0002-3613-3935>

[https://scholar.google.com/scholar?hl=id&as\\_sdt=0 %2C5&q=andy+erwin+wijaya&btnG=](https://scholar.google.com/scholar?hl=id&as_sdt=0%2C5&q=andy+erwin+wijaya&btnG=)

Ade Indra

Doctor Cand. (Ph.D.), Associate professor

Department of Mechanical Engineering

Institut Teknologi Padang (ITP)

Jl. Gajah Mada Jl. Kandis Raya, Kp. Olo, Kec. Nanggalo, Kota Padang, West Sumatera Barat, Indonesia, 25173

E-mail: [adeindra@itp.ac.id](mailto:adeindra@itp.ac.id)

Contact phone: +6281363243101

The number of articles in international databases: 2

H-index: 1

ORCID: <https://orcid.org/0000-0003-3048-4758>

<https://www.researchgate.net/scientific-contributions/Ade-Indra-2120638266>

Hendriwan Fahmi

Master of Mechanical Engineering, Associate Professor  
Department of Mechanical Engineering  
Institut Teknologi Padang (ITP)  
Jl. Gajah Mada Jl. Kandis Raya, Kp. Olo, Kec. Nanggalo, Kota Padang, West  
Sumatera Barat, Indonesia, 25173  
E-mail: [hendriwan\\_f@yahoo.com](mailto:hendriwan_f@yahoo.com)  
Contact phone: +6281363265251  
The number of articles in international databases: 4  
H-index: 2  
ORCID: <https://orcid.org/0000-0002-8129-4316>  
[https://www.researchgate.net/profile/Hendriwan\\_Fahmi](https://www.researchgate.net/profile/Hendriwan_Fahmi)

Yen-Pei Fu  
Doctor of Materials, Professor  
Department of Materials Science and Engineering  
National Dong Hwa University  
Shoufeng Township, Hualien, Taiwan ROC, 97401  
E-mail: [ypfu@mail.ndhu.edu.tw](mailto:ypfu@mail.ndhu.edu.tw)  
Contact phone: + 886-3-8634212  
The number of articles in international databases: 147  
H-index: 24  
ORCID: <https://orcid.org/0000-0002-2472-4981>  
[https://www.researchgate.net/profile/Yen-Pei\\_Fu](https://www.researchgate.net/profile/Yen-Pei_Fu)  
[researchgate.net/profile/Yen-Pei\\_Fu](https://www.researchgate.net/profile/Yen-Pei_Fu)